Article

Synthesized Bis-Triphenyl Phosphonium-Based Nano Vesicles Have Potent and Selective Antibacterial Effects on Several Clinically Relevant Superbugs

Silvana Alfei *, Guendalina Zuccari *, Francesca Bacchetti, Carola Torazza, Marco Milanese, Carlo Siciliano, Constantinos M. Athanassopoulos, Gabriella Piatti, Anna Maria Schito

Posted Date: 11 July 2024

doi: 10.20944/preprints202407.0891.v1

Keywords: multi-drug-resistant bacteria; triphenyl phosphonium salts; mitochondria target bola-amphiphiles; membranes permeabilization; MICs determination; time-killing experiments; cytotoxicity studies

Article

Synthesized *Bis*-Triphenyl Phosphonium-Based Nano Vesicles Have Potent and Selective Antibacterial Effects on Several Clinically Relevant Superbugs

Silvana Alfei [1,*], Guendalina Zuccari [1,2,*], Francesca Bacchetti [1], Carola Torazza [1], Marco Milanese [1,3], Carlo Siciliano [4], Constantinos M. Athanassopoulos [5], Gabriella Piatti [6] and Anna Maria Schito [6]

1 Department of Pharmacy, University of Genoa, Viale Cembrano, 16148 Genoa, Italy; francesca.bacchetti@edu.unige.it (F.B.); carola.torazza@unige.it (C.T.); marco.milanese@unige.it (M.M.)
2 Laboratory of Experimental Therapies in Oncology, IRCCS Istituto Giannina Gaslini, Via G. Gaslini 5, 16147, Genoa, Italy
3 IRCCS Ospedale Policlinico San Martino, Genova, Italia
4 Department of Pharmacy, Health and Nutritional Sciences, University of Calabria, 87036, Arcavacata of Rende, Italy; carlo.siciliano@unical.it
5 Department of Chemistry, University of Patras, University Campus Rio Achaias, 26504 Greece; kath@chemistry.upatras.gr (C.M.A.)
6 Department of Surgical Sciences and Integrated Diagnostics (DISC), University of Genoa, Viale Benedetto XV, 6, I-16132 Genova, Italy; amschito@unige.it (A.M.S); gabriella.piatti@unige.it (G.P.)
* Correspondence: alfei@difar.unige.it; Tel.: +39 010 355 2296 (S.A.); guendalina.zuccari@unige.it (G.Z.)

Abstract: The increasing emergence of multidrug resistant (MDR) pathogens, due to antibiotics misuse, translates in obstinate infections, with high morbidity and high-cost hospitalizations. To oppose these MDR superbugs, new antimicrobial options are necessary. Although both quaternary ammonium (QASs) and phosphonium salts (QPSs) possess antimicrobial effects, QPSs have been studied at lesser extent. Recently, we have successfully reported on the bacteriostatic and cytotoxic effects of a triphenyl phosphonium salt against MDR isolates of *Enterococcus* and *Staphylococcus* genus. Here, aiming at finding new antibacterial devices possibly bactericidal towards a broader spectrum of clinically relevant bacteria, responsible for severe human infections, we synthesized a water-soluble, sterically hindered quaternary phosphonium salt (BPPB). It encompasses two triphenyl phosphonium groups linked by a C12 alkyl chain, thus embodying the characteristics of molecules known as bola-amphiphiles. BPPB was characterized by ATR-FTIR, NMR and UV spectroscopy, FIA-MS (ESI), elemental analysis and potentiometric titrations. Optical and DLS analyses evidenced BPPB tendency to self-forming spherical vesicles in solution (45 nm by DLS), having a positive zeta potential (+18 mV). The antibacterial effects of BPPB were for the first time assessed against fifty clinical isolates of both Gram-positive and Gram-negative species. Excellent antibacterial effects were observed on all strains tested, involving all the most worrying species included in ESKAPE bacteria. The lowest MICs were 0.250 μg/mL, while the highest ones (32 μg/mL) were observed on MDR Gram-negative metallo-β-lactamase-producing bacteria and/or species resistant also to colistin, carbapenems, cefiderocol, so that intractable with current available antibiotics. Moreover, when administered to HepG2 human hepatic and Cos-7 monkey kidney cell lines, BPPB showed selectivity indices > 10 for all Gram-positive isolated and for clinically relevant Gram-negative superbugs such as those of *E. coli* species, thus being very promising to be clinically developed.

Keywords: multi-drug-resistant bacteria; triphenyl phosphonium salts; mitochondria target bola-amphiphiles; membranes permeabilization; MICs determination; time-killing experiments; cytotoxicity studies

 doi:10.20944/preprints202407.0891.v1

1. Introduction

Multi drug resistant (MDR) bacteria, such as ESKAPE pathogens, being ESKAPE the acronym for *Enterococcus faecium, Staphylococcus aureus, Klebsiella pneumoniae, Acinetobacter baumannii, Pseudomonas aeruginosa,* and *Enterobacter* species, are an irrepressible worldwide threat to both humans and animals and a global public health problem [1]. Their control using the currently available antibiotics represents a daily challenge for experts in the field, being them no longer functioning, or functioning at very high dosages, which, paradoxically, can promote the emergence of additional forms of resistance. These MDR pathogens are therefore responsible for difficult-to-treat infections, with long-term hospitalizations, high management costs, and cause approximately 35,000 deaths per year in the United States [2]. Such global antibiotic resistance crisis could be limited by reducing the misuse of antibiotics both in medicine, agriculture and in the environment [3], as well as by performing an efficient infection control strategy to prevent the spread of contagions [2]. [4,5]. Even, under biofilm conditions, a higher dosage of antibiotics is necessary, which absurdly drives to further antibacterial resistance [3].

In case of bacterial resistance to available antibiotics, alternative treatments that can improve their efficacy, such as the use of metabolites (L-alanine and glucose) capable of modifying the bacteria metabolism or of nanomaterial-based delivery systems, could allow to reduce the amounts of antibiotics necessary to counteract infections, thus limiting the further emergence of resistance in pathogens [6]. Several new agents based on existing classes of antibiotics, such as cefiderocol from cephalosporins, omadacycline from tetracycline and vancomycin A from vancomycin, are being developed [6], but the exclusive discovery of novel agents is still inadequate [3]. New antibacterial drugs are searched by exploring peculiar sources, such as soil actinomycetes, insects, marine samples, or microbiota, as well as by screening small-molecule libraries [6]. Anyway, such libraries typically contain more than 10,000 synthetically produced chemical compounds, and the probability for a new molecule to become a clinically applicable drug is only 1:10,000. In this regard, a new lead antibiotic was identified by screening 167,405 compounds, which demonstrated to possess inhibiting effects against methicillin-resistant *S. aureus* (MRSA) and vancomycin-resistant *S. epidermidis* (VRE), but no effect was observed against Gram-negative bacterial pathogens, which remain the most concerning [7].

An entirely novel treatment characterized by a unique mechanism of action, with no tendency to develop resistance, is represented by antimicrobial oxidative therapy (AOT) through induction of reactive oxygen species (ROS) by different methods [3,8].

As reported, ROS have demonstrated *in vitro* and *in vivo* significant antimicrobial properties against a wide spectrum of Gram-positive, Gram-negative organisms, fungi, and parasites, including MDR isolates and biofilm-producing pathogens [9]. Anyway, to date, ROS could represent a new therapeutic approach only for topical use on skin, mucosal membranes, or internal tissue [10]. Although treatments involving ROS as antimicrobial agents are already clinically approved to treat infected wounds, including chronic wounds, superficial and acute wounds, burns, surgical wounds, cuts, abrasions, and diabetic foot ulcers, they are not suitable for systemic use, so far [11]. Further clinical investigations are mandatory on the possible toxic effects of ROS on mammalian cells [8].

Concerning synthetic compounds promising as new possible antibacterial agents, cationic surfactants, namely quaternary heteronium salts, including quaternary ammonium salts (QASs) derivatives of benzalkonium chloride (CITROSIL®), have been studied since 1930 [12]. QASs demonstrated considerable broad-spectrum potency and biocidal effects against Gram-positive and Gram-negative bacteria, some fungi, parasites, and even enveloped lipophilic viruses [13,14]. Their antimicrobial activity depends mainly on the charge, the number of cationic centers, the nature of the counter-ion, the length and number of alkyl substituents and the possible presence of aromatic groups [15].

As the chain length of alkyl groups increases, the biological activity of the compounds increases up to a critical point, beyond which the activity is lost [1]. Although some additional possible mechanisms for these biocides have been proposed [16], they generally disrupt the cell membranes of micro-organisms [17,18]. Upon the incorporation of their long lipophilic substituents and the

 doi:10.20944/preprints202407.0891.v1

cationic center(s) into the phospholipid bilayer, they destroy the cell membrane and act on bacteria regardless of their specie and/or pattern of resistance [18]. Specifically, after electrostatic interaction with the external negative constituents of bacteria, by intercalating into the membranes, altering their normal structure, and causing depolarization, QASs succeed in modifying membranes permeability by pores formation, thus determining the loss of ions, enzymes, and coenzymes. The biosynthetic activity of bacteria results irreversibly compromised, thus prompting their death [13,19,20]. Due to these actions, QASs demonstrated to be active against worrying MDR strains such as *E. faecium, S. aureus, K. pneumoniae, A. baumannii* and *P. aeruginosa* [21].

On the other hand, the non-specific antimicrobial mechanism of QASs may decode for a low discrimination for pathogens. Their noteworthy cytotoxicity and hemolytic toxicity on eukaryotic cells [13,22,23] impede their oral and systemic administration *in vivo*, thus limiting their use as surfaces disinfectants and antibacterial devices for topical treatment [17].

A more recently studied class of quaternary heteronium salts, structurally like QASs and with similar biological properties, investigated from the middle of the 20th century, consists of quaternary phosphonium salts (QPSs) [24–26]. Despite their similarities with QASs, QPSs have shown higher biological activities, including antibacterial and antitumor effects than QASs, because of a difference of electronegativity between phosphorous and carbon atoms [20,27,28]. On the contrary, lower cytotoxicity was observed for QPSs with respect to structurally analogous QASs [28,29]. It has been reported that QPSs with C8-C11 alkyl chains have significant and discerning antibacterial effects especially against Gram-positive species [30,31].

Intensive research has been performed on the antibacterial activity of a series of tri-*n*-hexyl-(alkyl)-phosphonium ionic liquids (PILs), with alkyl chains of diverse lengths and different anions by Seddon et al., thus finding that the antimicrobial properties of such PILs is based on the alkyl substituent length and depends on the type of anion [31]. Phosphonium compounds have also been covalently bonded to plastic surfaces or used as co-extrusive additives for plastic materials which have demonstrated antibacterial properties [32,33]. Anyway, the optimization of the balance between antimicrobic activity and cytotoxicity, and the development of strategies to regulate the biological properties of QPSs, through structural tuning, is still needed In this context, the peculiar structure of the sterically hindered phosphonium salts (HPSs), the charge distribution of their cation(s) and the shielding of charged phosphorus atoms by hindering groups could allow the hypothesis that such compounds could possess distinctive biological properties and different mechanisms of interaction with living cells, with a possible reduced hemolytic toxicity and cytotoxicity [1].

HPSs with three *tert*-butyl and three phenyl residues have been studied. Ermolaev et al studied for the first time the structure-activity relationships of tri-*tert*-butyl phosphonium salts having form C1 to C20 alkyl chains and bromide, iodide or BF_4^- anions [1].

When tested on *S. aureus, Bacillus cereus, E. faecalis, E. coli, P. aeruginosa*, as well as MRSA isolates resistant to fluoroquinolones and/or β-lactams and some fungi, compounds with C11 to C18 chains demonstrated from good to excellent antimicrobial effects [1]. Interestingly, the investigated phosphonium salts demonstrated high antimicrobial activity and selectivity for bacteria, as well as were safe for normal human cells [1]. Hindered QPSs based on triphenylphosphine have been studied to an even greater extent, thus evidencing a broad spectrum of biological activities, and antifouling properties [12]. Recently, we have reported on the remarkable bacteriostatic activity (MICs = 4–16 μg/mL), and controlled cytotoxicity of a triphenyl phosphonium salt bearing a C10 1-hydroxyl chain [12]. It was specifically active against MDR isolates of *Enterococcus* and *Staphylococcus* genus [12]. At the lower MIC concentration, this compound did not show significant cytotoxic effects when exposed to HepG2 human hepatic cell lines, paving the way for its potential clinical application [12]. *Bis* (triphenyl phosphonium) salts (BTPPSs), which could include bola-amphiphiles (a class of surfactants featuring one or more hydrophobic chains that connect two identical or different hydrophilic headgroups) have shown sterilizing properties [34,35] and antibacterial activity higher than that of mono triphenyl phosphonium salts and low levels of cytotoxicity [36,37]. This major antibacterial activity and low cytotoxicity could be attributable to the presence of more than one

 doi:10.20944/preprints202407.0891.v1

cationic moiety and to the "soft" cationic nature of the headgroups, characterized by an extended delocalization of the positive charge on the phenyl rings, respectively [38]. This all translates into a greater ability of these substances to interact and cross membranes with highly negative potential, such as those of bacteria, damaging them and facilitating their entry into the cell [38]..Due to the difference in negative electrical membrane potentials between bacterial and normal cells, these compounds selectively interact and accumulate within bacterial membranes and cells compared to those of mammals [36]. Once inside the bacterial cell, BTPPSs can detrimentally interact with other negative constituents, including genomic and plasmid DNA, thus causing bacterial death [30]. With these premises, we aimed at finding new antibacterial devices with a broader spectrum of antibacterial effects than that of the recently reported phosphonium salt [12], finalized at counteracting human and animal infections sustained by MDR Gram-positive and Gram-negative strains, no longer treatable with available antibiotics. To this end, we synthesized and characterized a water-soluble sterically hindered quaternary phosphonium salt (BPPB), possessing two triphenyl phosphonium groups linked by a C12 alkyl chain (Figure 1).

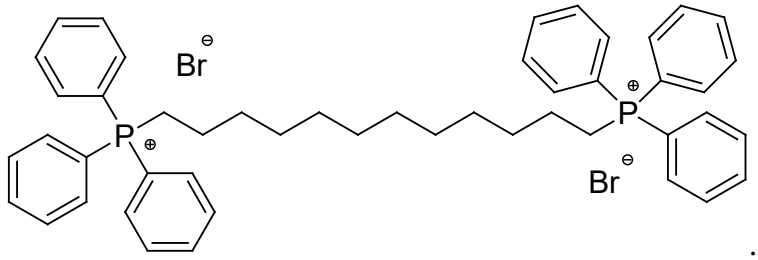

Figure 1. Chemical structure of the BPPB.

Although it had already been reported in terms of synthetic procedures, colloidal properties [38]and sterilizing effects, these were only assessed on environmental bacteria. On the contrary, it was never tested on clinically relevant superbugs responsible for almost intractable human and animal infections [34,35], and its cytotoxic effects on eukaryotic cells were never investigated. BPPB was characterized by ATR-FTIR, NMR and UV spectroscopy, FIA-GC (ESI), and elemental analysis to confirm its structure. Potentiometric titrations, optical microscopy and DLS analyses were also carried out. For the first time, the antibacterial effects of BPPB were assessed against a multitude (50 strains) of clinical isolates of different genus of both Gram-positive and Gram-negative species, all with difficult to manage patterns of resistance. To this end, MICs determinations were carried out with BPPB on all isolates considered in this study, while 24-hours time killing experiments were performed on different strains of *E. coli* and MRSA, as representative isolates of Gram-positive and Gram-negative species. Moreover, for the first time, cytotoxicity experiments were also performed, using HepG2 human hepatic and Cos-7 monkey kidney cells as *in vitro* models to establish the potential clinical application of BPPB.

2. Materials and Methods

2.1. Chemicals and Instruments

All reagents and solvents were from Merck (formerly Sigma-Aldrich, Darmstadt, Germany) and were purified by standard procedures. The organic solutions were were evaporated using a rotatory evaporator operating at a reduced pressure of about 10–20 mmHg. The melting range of BPPB was determined on a 360 D melting point device with a resolution of 0.1 °C (MICROTECH S.R.L., Pozzuoli, Naples, Italy). The melting point is uncorrected. Attenuated total reflectance (ATR) Fourier transform infrared (FTIR) analyses were carried out on the same instrument as previously reported [39]. ^{1}H , ^{13}C and ^{31}P NMR spectra of PBBP were acquired on a Jeol 400 MHz spectrometer (JEOL USA, Inc., Peabody, MA, USA) at 400, 100 and 162 MHz, respectively. Standard ^{13}C NMR spectra were reported. Chemical shifts were reported in ppm (parts per million) units relative to the internal standard tetramethylsilane (TMS = 0.00 ppm)., and the splitting patterns were described as follows:

Preprints.org (www.preprints.org) | NOT PEER-REVIEWED | Posted: 11 July 2024 doi:10.20944/preprints202407.0891.v1

s (singlet), d (doublet), t (triplet), q (quartet), m (multiplet), and br (broad signal). FIA-MS experiments were performed on a linear ion trap mass spectrometer (LXQ Thermo Finningan, Thermofisher, Italy, PR) equipped with a heated electrospray ionization (HESI) source. Operating conditions of the HESI were as follows: source temperature: 50 °C; ion spray voltage = +4.0 kV; sheath gas = 5 (arbitrary scale); capillary temperature = 275 °C. Methanolic solutions of samples (1×10^{-5} M) were infused via a syringe pump at a flow rate of 3–5 µL/min. Potentiometric titrations were carried out using a Hanna Micro-processor Bench pH Meter (Hanna Instruments Italia srl, Ronchi di Villafranca Padovana, Padova, Italy) in mV mode, which was calibrated using standard solutions at pH = 4, 7, and 10 before titrations. Elemental analyses were carried out using an Elemental Analyzer (Fison Instruments Ltd., Farnborough, Hampshire, England). Thin layer chromatography (TLC) was performed using aluminum-backed silica gel plates (Merck DC-Alufolien Kieselgel 60 F254, Merck,Washington, DC, USA), and detection of spots was made by UV light (254 nm) using a Handheld UV Lamp, LW/SW, 6W, UVGL-58 (Science Company®, Lakewood, CO, USA).

2.2. Synthesis of 1,1-(1,12-dodecanediyl)bis [1,1,1]-triphenylphosphonium di-Bromide (BPPB)

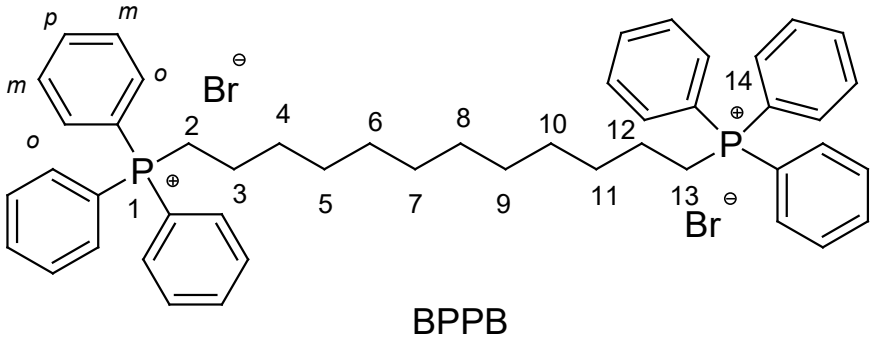

BPPB

Figure 2. Chemical structure of the BPPB with atoms numbering for NMR peaks assignation.

1,12-dibromo-dodecane (1.00 g, 0.003 moles) and triphenylphosphine (TPP) (1.60 g, 0.006 moles) were dissolved in 30 mL ethanol (EtOH). The reaction mixture was kept under stirring and refluxed for 48 h: Then, the solvent was removed under vacuum, obtaining a yellowish resin which was recrystallized by q.b. dichloromethane (DCM)/di-isopropyl ether (DIPE) as couple solvent/non-solvent obtaining a white precipitate, which was separate by filtration, washed twice with diethyl ether (Et_2O) and brought to constant weight at reduced pressure. The final product was obtained as hygroscopic low-melting point white foam (2.18 g, 0.0026 moles, 85.2%). M. p. < 70 °C. ATR-FTIR (ν, cm^{-1}): 3052, 3007 (C-H stretching phenyl rings), 2923 (CH_2), 2852 (CH_2), 1586, 1484 (C=C stretching), 1436, 995 (aromatic C-P), 689 (aliphatic C-P). ^{1}H-NMR (400 MHz, $CDCl_3$) ppm: 1.16 (m, 4H, [6,9] CH_2), 1.22 (m, 4H, [5,10] CH_2), 1.23 (m, 4H, [7,8] CH_2), 1.50 (m, 4H, [4,11] CH_2), 1.60 (m, 4H, [3,12] CH_2), 3.62 (dt, 4H, [2,13] CH_2, $J_{CH2(2,13)\text{-}P}$ = 13.0 Hz, J = 6.20 Hz), 7.63 (m, 12H, *meta* ArH), 7.67 (m, 6H, *para* ArH), 7.95 (m, 12H, *orto* ArH). ^{13}C-NMR (100 MHz, $CDCl_3$) ppm: 21.94 (2d, [3,12] C); 22.26 (2d, [2,13] C, $J_{C(2,13)\text{-}P}$ = 50.10 Hz); 28.60 (2s, [7,8] C); 29.39 (2d, [6,9] C); 29.55 (2d, [5,10] C); 30.17 (2d, [4,11] C); 118.32 (6d, ArC-P, $J_{ArC\text{-}P}$ = 86.0 Hz); 130.09 (12d, ArCH*orto*, $J_{ArCH\textit{orto}\text{-}P}$ = 12.5 Hz); 133.53 (12d, ArCH*meta*, $J_{ArCH\textit{meta}\text{-}P}$ = 10.2 Hz); 134.72 (6s, ArCH*para*). ^{31}P-NMR (162 MHz, $CDCl_3$) ppm: 26.72 (s, P nuclei 1,14). FIA-MS-(ESI): 346.25 m/z $[C_{48}H_{54}P_2]^{2+}$. Anal. Calcd. for $C_{48}H_{54}P_2Br_2$: C, 64.61; H, 6.38; P, 7.26. Found: C, 64.63; H, 6.41; P, 7.30.

2.3. UV-Vis Analyses

The UV-Vis spectrum of BPPB was acquired in water at room temperature. BPPB (6.8 mg) was disolved in 0.5 mL water by gently heating, obtaining a clear solution 13.6 mg/mL (15.9 mM). 220 µL were withdrawn and diluted to 50 mL to obtain a solution at concentration like that reported by Cecacci et al [38]. The obtained solution was analyzed using an Agilent Cary 100 UV/Vis Spectrophotometer (Agilent Technologies Italia S.p.A., Milan, Italy). Analyses were performed in triplicates and the image reported in the Results and Discussion section is a representative acqisition.

 doi:10.20944/preprints202407.0891.v1

2.4. Potentiometric Titration of BPPB

The potentiometric titration of BPPB was carried out in a mixture of anhydrous acetic acid (AcOH) and acetic anhydride (Ac_2O) 30:70 (v/v)), with $HClO_4$, performing a procedure previously described by us for the volumetric titration of primary ammonium salts, slightly modified [40–42]. The protocol was first described by Pifer and Wollish for titrating quaternized ammonium salts [43]. Succinctly, an exacted weighted sample of BPPB (280.0 mg) was dissolved in AcOH/Ac_2O 30/70 (5 mL), treated with 2-4 mL of a solution of mercury acetate (1.5 g) in AcOH (25 mL), and titrated with a standardized 0.1 N solution of $HClO_4$ in AcOH/Ac_2O, prepared as described in the following section, using potentiometric endpoint detection. The titrations were performed under efficient stirring with a magnetic stirrer, at room temperature (25 ± 2 ◦C). Millivolts were measured every 0.5 mL up to 6 mL and every 0.1 mL in the vicinity of the calculated endpoint up to the addition of 8 mL 0.1 N $HClO_4$. Titrations were made in triplicate, and the measurements were reported as mean ± SD.

2.4.1. Preparation of 0.1 M Perchloric Acid Volumetric Solution

The 0.1 M perchloric acid volumetric solution was prepared by diluting 8.5 mL of 70–73 wt% perchloric acid with 900 mL of anhydrous acetic acid and 30 mL of acetic anhydride and then diluting to 1000 mL with anhydrous acetic acid. Perchloric acid was standardized by titration against potassium hydrogen phthalate.

2.5. Optical Microscopy Analyses

The morphology of BPPB as water suspension was investigated via optical microscopy (OM) analysis. In the performed experiments, 6.8 mg of solid BPPB were dissolved in 0.5 mL water by gently heating, obtaining a clear solution 13.6 mg/mL (15.9 mM). The fine suspension obtained on cooling was observed using a Leica DM750 optical microscope (Leica Italy, Milan, Italy) equipped with 40 ×, and 100 × objectives. The camera used for image capture was a Leica ICC50W (Leica Italy, Milan, Italy). All images were processed using LAS EZ 3.4.0. software (Leica Italy, Milan, Italy).

2.6. Dynamic Light Scattering (DLS) Analysis

The particle size (nm) intended as hydrodynamic diameter distribution, polydispersity index (PDI), and zeta potential (ζ-p) (mV) of BPPB were measured at 25 °C, at a scattering angle of 90° in m-Q water by using a Malvern Nano ZS90 light scattering apparatus (Malvern Instruments Ltd., Worcestershire, UK).

A solution of BPPB 10 mM in m-Q water (312.4 Kcps) was diluted 1:2 to reach the final concentration of 5 mM (8.4 kcps) and analyzed. The ζ-p value of BPPB was recorded with the same apparatus at count rate 20-59 kcps. The results of experiments were presented as the mean of 3 independent determinations, made of 10 runs (particle size) or 12 runs (ζ-p), each one ± SD. Intensity-based results were reported to express the particle size distribution.

2.7. Microbiology

2.7.1. Microorganisms

A total of 50 isolates, belonging to a collection of MDR Gram-positive and Gram-negative species of the University of Genova, were used in this study. All were clinical strains isolated from human specimens and identified by VITEK® 2 (Biomerieux, Firenze, Italy) or matrix-assisted laser desorption/ionization time-of-flight (MALDI-TOF) mass spectrometric technique (Biomerieux, Firenze, Italy). The 50 MDR isolates included 22 Gram-positive and 28 Gram-negative bacteria of different genus. Among bacteria of Gram-positive species, 8 were enterococci (4 *E. faecalis* and 4 *E. faecium*), while 14 were staphylococci (8 *S. aureus* and 6 *S. epidermidis*). All enterococci were MDR isolates, with resistance to vancomycin (VRE), while all staphylococci were MDR strains with resistance to methicillin (MRSA and MRSE). Additionally, three MRSE (*S. epidermidis*) displayed resistance also to linezolid. Gram-negative species included non-fermenting isolates such as *P.*

 doi:10.20944/preprints202407.0891.v1

aeruginosa (4 isolates), *A. baumannii* (5 strains), and *Stenotrophomonas maltophylia* (5 isolates), as well as *Enterobacteriaceae*, such as *E. coli* (5 isolates), *K. pneumoniae* (5 strains) *Klebsiella aerogenes* (1 isolate), 2 isolates of *Enterobacter cloacae* and 1 isolate of *Enterobacter hormaechei*. Among 4 *P. aeruginosa,* 3 were isolated from cystic fibrosis patients and were resistant to carbapenems. Two of them were also pyoverdine and pyocyanin producers, while one was ceftazidime-avibactam (CAZAVI) resistant. The fourth *P. aeruginosa* was a MDR isolate resistant also to colistin. All five *A. baumannii* were carbapenems resistant MDR isolates, while the five *S. maltophylia* were MDR strains of which 1 was resistant also to cotrimoxazole (trimethoprim and sulfamethoxazole). Except for one *E. coli* which was fully sensitive, all the residual 4 *E. coli* and all the five *K. pneumoniae* were resistant to carbapenems. Four *K. pneumoniae* were KPC producers, one of which was also colistin-resistant, while 1 was metallo-β-lactamese VIM-1 producer, with resistance also to the recently approved cefiderocol. Among MDR *E. coli*, two were producers of the New Dheli metallo-β-lactamese (NDM), one of which displayed resistance also to cefiderocol, one was VIM-1 producer, while the last *E. coli* was a KPC producer isolate. *K. aerogenes* was a KPC producer isolate, *E. cloacae* isolates were VIM-1 producers, while *E. hormaechei* demonstrated resistance also to cefiderocol.

2.7.2. Determination of the MICs

To investigate the antimicrobial activity of BPPB on the described pathogens, their Minimal Inhibitory Concentrations (MICs) were determined by following the microdilution procedures detailed by the European Committee on Antimicrobial Susceptibility Testing EUCAST [44], and reported in our previuos works [12].

2.7.3. Killing Curves

Killing curve assays for BPPB were carried out on isolates of *S. aureus* (strain 17, 18, 187 and 195, all MRSA), and *E. coli* (strains 477, 525 and 539), following a procedure previously reported [45]. Experiments were performed over 24 h at BPPB concentration of four times the MIC for all strains.

A mid logarithmic phase culture was diluted in Mueller–Hinton (MH) broth (Merck, Darmstadt, Germany) (10 mL) containing 4 × MIC of the selected compound to give a final inoculum of 1.0×10^5 CFU/mL. The same inoculum was added to cation-supplemented Mueller–Hinton broth (CSMHB) (Merck, Darmstadt, Germany), as a growth control. Tubes were incubated at 37 °C with constant shaking for 24 h. Samples of 0.20 mL from each tube were removed at 0, 2, 4, 6, and 24 h, diluted appropriately with a 0.9% sodium chloride solution to avoid carryover of BPPB being tested, plated onto MH plates, and incubated for 24 h at 37 °C. Growth controls were run in parallel. The percentage of surviving bacterial cells was determined for each sampling time by comparing colony counts with those of standard dilutions of the growth control. Results have been expressed as log10 of viable cell numbers (CFU/mL) of surviving bacterial cells over a 24-hour period. Bactericidal effect was defined as a 3 log10 decrease of CFU/mL (99.9% killing) of the initial inoculum. All time-kill curve experiments were performed at least in triplicate.

2.8. Concentration-Dependent Cytotoxicity Experiments: MTT and LHD Tests

2.8.1. MTT cytotoxicity assay

To assess the cytotoxicity properties of PBBP, the MTT (3-(4,5-dimethylthiazol-2-yl)-2,5-diphenyltetrazolium bromide) cell proliferation assay [46] (Abcam, Cat#ab2011091) was performed, following the manufacturer's protocol, as previously reported [12]. Briefly, Cos-7 cells (African green monkey kidney fibroblast-like cell line) and HepG2 cells (human liver epithelial-like cell line) were plated at 20.000 cells/well into 96-well plates, the cells were maintained in complete Dulbecco's Modified Eagle Medium (DMEM; Euroclone, Cat# ECM0728L) containing 10% Fetal Bovine Serum (Euroclone, Cat# ECS0180L), 1% glutamine (Euro-clone, Cat# ECB3004D) and 1% Penicillin/Streptomycin (Euroclone, Cat# ECB3001D) at 37°C, in 5% CO_2 atmosphere for 24 h. Once verified the optimal cell confluence, the complete DMEM was replaced with fresh media containing increasing concentrations of bis-phosphonium bromide (range of 0.5-100 μg/mL), and the cells were

 doi:10.20944/preprints202407.0891.v1

incubated at 37°C in 5% CO_2 for further 24 h. After that, the media was removed, and cells were washed with PBS. Aliquots (200 µL) of serum-free medium containing MTT (Merck, Cat #M5655; 0.25 mg/mL MTT) were added to each well and incubated at 37 °C for 3h. After removing the medium, 200 µL of DMSO solution (Merck, Cat #276855; 0.25 mg/mL MTT) was added to each well and horizontally shaken for 10 min to allow DMSO to solubilize the formazan crystals, allowing the formation of a homogenous solution. The 570 nm wavelength light absorption was then measured spectrophotometrically in each well, by using the Spectra Max 340 PC (Molecular Devices, San Jose, California, US), and converted in OD (optical density) units. The cell survival rate, expressed as cell viability percentage (%), was evaluated based on the experimental outputs of treated groups vs. the untreated groups (CTR) and was calculated as follows: cell viability (%) = (OD treated cells − OD blank)/(OD untreated cells − OD blank) × 100%.

2.8.2. LDH cytotoxicity assay

To assess the cytotoxicity properties of bis-phosphonium bromide, the lactate dehydrogenase (LDH) cytotoxicity assay [47] (Abcam, Cat#ab102526) was performed, following the manufacturer's protocol. Briefly, Cos-7 and HepG2 cells were seeded at 20.000 cells/well into 96-well plates, the cells were maintained in complete Dulbecco's Modified Eagle Medium (DMEM; Euroclone, Cat# ECM0728L) containing 10% Fetal Bovine Serum (Euroclone, Cat# ECS0180L), 1% glutamine (Euroclone, Cat# ECB3004D) and 1% Penicillin/Streptomycin (Euroclone, Cat# ECB3001D) at 37°C in 5% CO_2 atmosphere for 24 h. Once verified the optimal cell confluence, the complete DMEM was replaced with fresh media containing increasing concentrations of bis-phosphonium bromide (range of 0.5-100 µg/mL), and the cells were incubated at 37°C in 5% CO_2 for further 24 h. After that, the supernatant medium was collected, and immediately transferred to new 96-well flat-bottom enzymatic assay plates. 50 µL of LDH assay substrate was added to the medium and the absorbance measure output was immediately recorded at 450 nm, by using a microplate reader (Spectra Max 340 PC, Molecular Devices, San Jose, California, US) set up in a kinetic mode, every 2–3 minutes, for at least 30 minutes at 37°C. Positive control outputs were used as the maximum LDH signal. The LDH content (OD at 450 nm) quantified in the cultured medium collected from treated or untreated conditions is directly proportional to damaged cells.

2.8.3. Statistics

Graphs and statistics were generated by GraphPad Prism (Version 9, license code GP9-2314983-RATL-05225; 225 Franklin Street. Fl. 26, Boston, MA, USA 02110; RRID:SCR_002798).

3. Results and Discussion

3.1. Synthesis of 1,1-(1,12-dodecanediyl)bis [1,1,1]-triphenylphosphonium di-Bromide (BPPB)

With the scope to develop novel antibacterial agents effective against MDR bacteria of both Gram-positive and Gram-negative species, and due to the reported antibacterial effects of QPSs [12,20,27,30,31], and those even superior of *bis*-(triphenyl-phosphonium) salts [36,37], we synthesized the dodecyl *bis*-triphenilphosphonium derivative (Figure 1) according to Scheme 1.

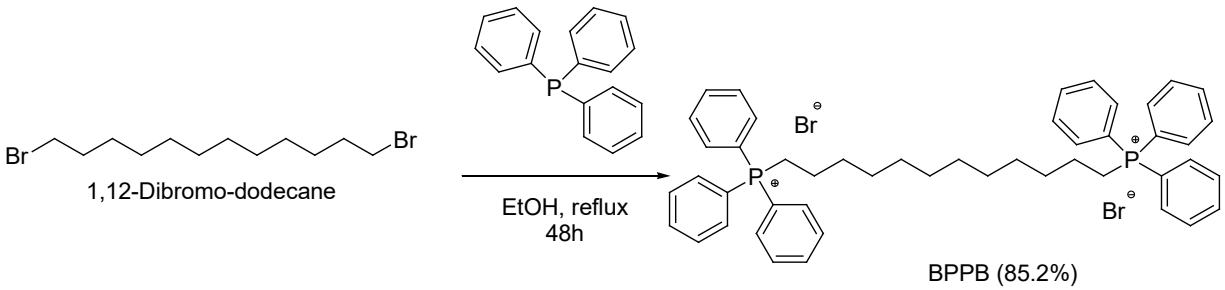

 doi:10.20944/preprints202407.0891.v1

Scheme 1. Synthetic route to achieve BPPB.

The C12 chain was selected, since among the hindered mono phosphonium bromides reported by Ermolaev et al. [1], bearing a C12 alkyl chain demonstrated very high antibacterial effects, very low level of hemotoxicity and little cytotoxicity to Chang liver cells. The C12 derivative demonstrated the highest selectivity index for bacteria *S. aureus* 209 P and MRSA compared to blood cells, also when used to coat polymer surfaces [1]. Additionally, even if only against environmental bacteria and never on MDR clinical isolates as made by us, the sterilizing action of *bis* phosphonium bola-amphiphilies bearing a C12 chain was reported [34,35]. EtOH was used as solvent in place of DMF used by Caccacci et al [38]to facilitate the solvent removal and void to retain residual DMF in the product. The reaction advancement was followed by TLC (AcOEt/Petrol ether 1/1) and it was stopped when the spot of triphenylphosphine (TPP, Rf = 0.25) disappeared. In this eluent mixture BPPB displayed Rf = 0. The pale yellow resin obtained by removing the solvent under pressure was recrystallized by diclholoromethane (DCM)/di-isopropyl ether (DIPE) obatining pure BPPB as low-melting-point white foamy solid with high tendency to absorb atmospheric humidity and in yield comparable [38]or even higher [34,35]than those previously reported. BPPB was characterized by ATR-FTIR (Figure 3), ^{1}H NMR (Figure 4), ^{13}C-NMR (Figure 5), ^{13}C-NMR DEPT 135 and ^{31}P-NMR spectroscopy (Figure 6), FIA-MS experiments, UV analyses, as well as elemental analyses which confirmed its structure and good degree of purity.

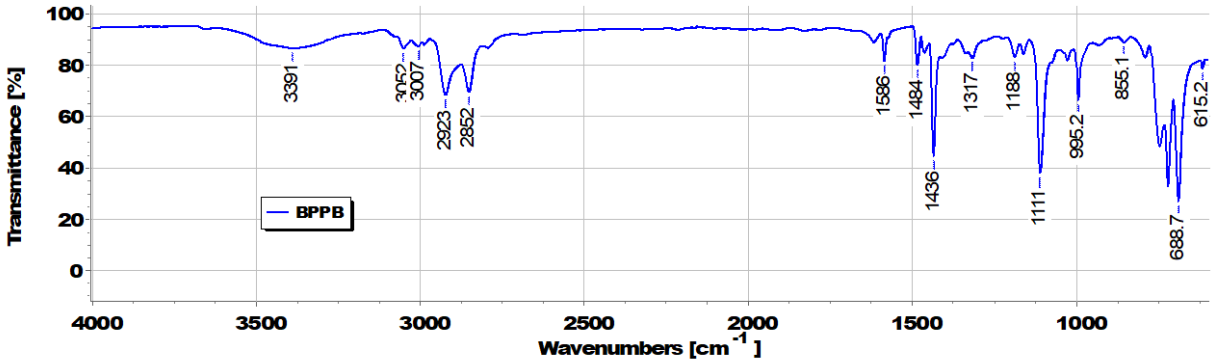

Figure 3. ATR-FTIR spectrum of BPPB.

Particularly, in the FTIR spectrum, the weak bands of the phenyls C-H stretching (3052 and 3007 cm^{-1}) were observable, while the bands of the symmetric and asymmetric stretching of C–H of the several methylene groups of the C12 alkyl chain were observable at 2923 and 2852 cm^{-1} respectively [48]. The band of the aliphatic C-P stretching was detected at 689 cm^{-1}, while two bands at 1436 and 995 cm^{-1} were observed for the aromatic C-P stretching [49]. The stretching vibrations bands of aromatic C=C bonds in the phenyl groups were instead visible at 1484 and 1586 cm^{-1} [35,48].

Preprints.org (www.preprints.org) | NOT PEER-REVIEWED | Posted: 11 July 2024 doi:10.20944/preprints202407.0891.v1

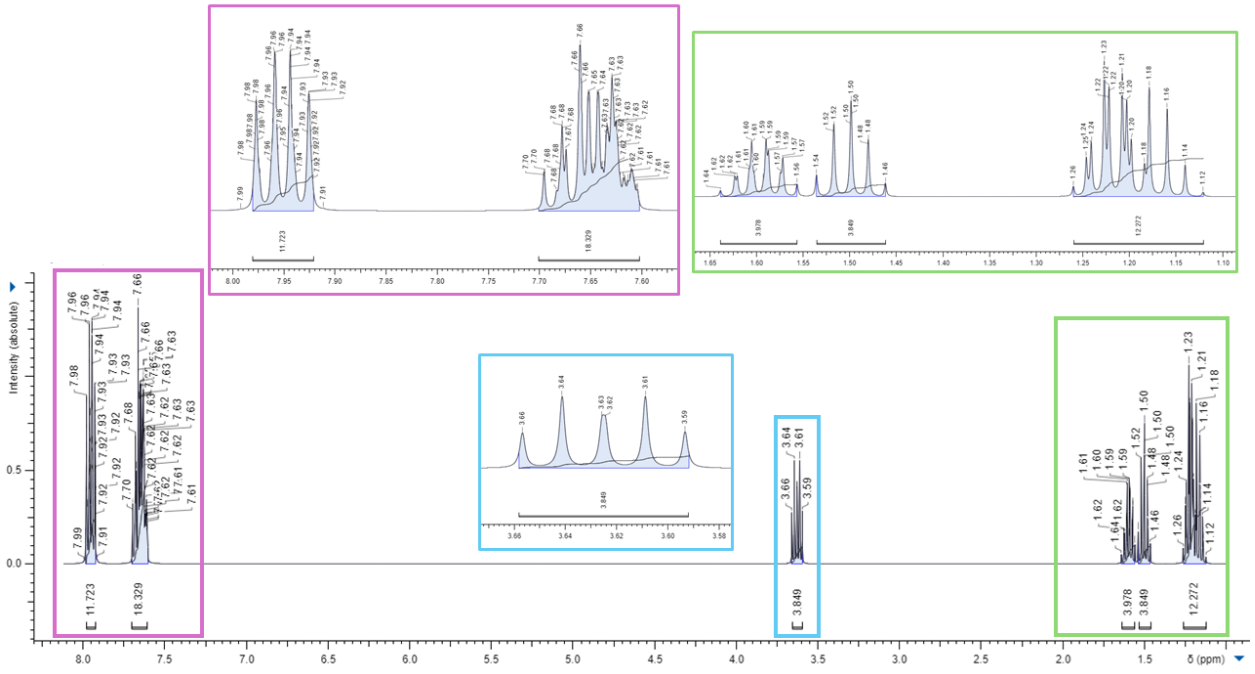

Figure 4. ^{1}H NMR spectrum ($CDCl_3$, 400 MHz) of BPPB. Signals in squares of the same color indicate the signals present in the original spectrum and its corresponding magnification.

The ^{1}H NMR spectrum of BPPB showed five broad multiplets in the range 1.16-1.60 ppm at 1.16, 1.22, 1.23, 1.50 and 1.60 integrable for 4H each one and belonging to the C4-C11 (see the numbered structure of BPPB in Figure 2) methylene groups. The signal of the CH_2-P^+ groups was instead detected as double triplet at 3.62 ppm whose multiplicity is due to the spin-spin coupling of protons with both the vicinal methylene group (J = 6.20 Hz) and with the phosphorus atom (J = 13.0 Hz). Finally, a complex signal made of three multiplets centered at 7.63, 7.67 and 7.95 ppm and integrable for 12H, 6H and 12H respectively was detected in the range 7.61-7.99 ppm due to the proton atoms of the six phenyl rings.

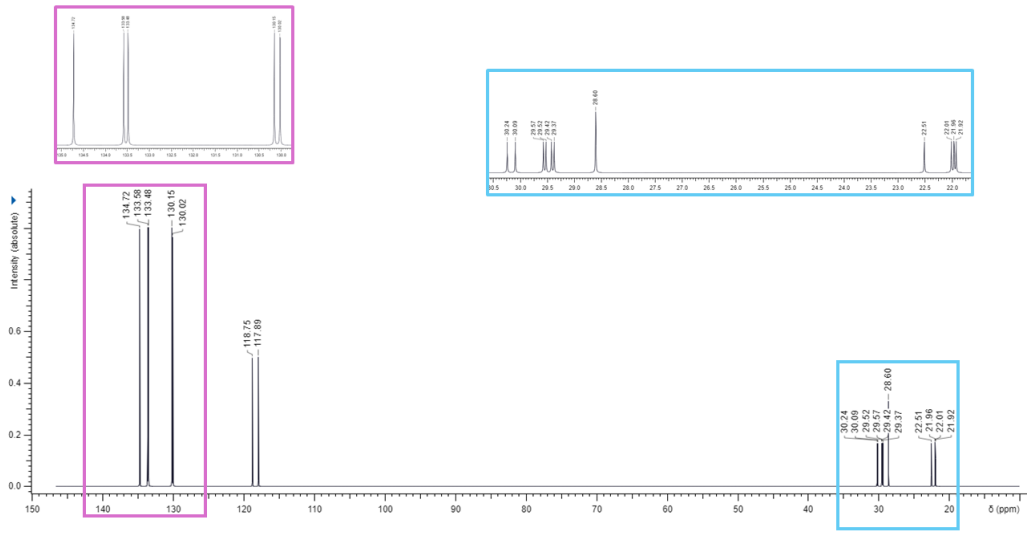

Figure 5. ^{13}C-NMR spectrum ($CDCl_3$, 100 MHz) of BPPB. Signals in squares of the same color indicate the signals present in the original spectrum and its corresponding magnification.

 doi:10.20944/preprints202407.0891.v1

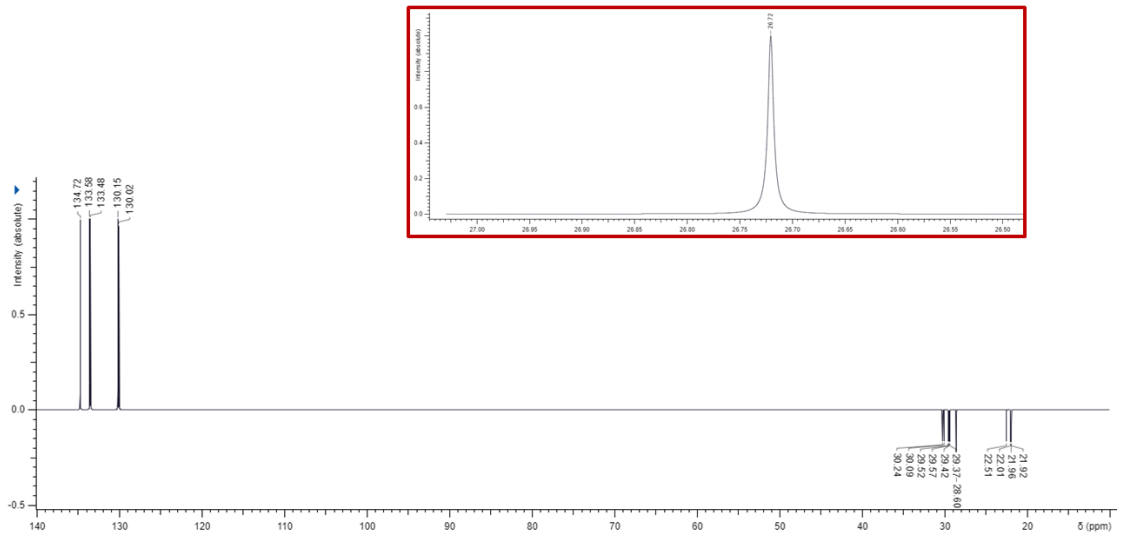

Figure 6. ^{13}C-NMR DEPT 35 spectrum ($CDCl_3$, 100 MHz) of BPPB and its ^{31}P-NMR spectrum ($CDCl_3$, 192 MHz) (red square).

At high fields (21.92-30.24 ppm) in the ^{13}C-NMR spectrum of BPPB, six signals due to the C2, C3, C4, C5, C6, C7, C8, C9, C10 and C11 (see the numbered structure of BPPB in Figure 2) methylene groups of the aliphatic chain were detected (Figure 5), which appeared downwards-oriented in the DEPT-135 analysis (Figure 6). Carbons spin-spin coupling with the phosphorous atom were observed for C2, C13 ($J_{C2,13\text{-}P}$ = 50.1 Hz), while no coupling was observed for other carbon atoms of the alkyl chain. The doublet signals of the quaternary carbon atoms of benzene rings directly bonded to P^+, which disappeared in the DEPT-135 analysis were found at 118.32 ppm, and showed a coupling constant $J_{C\text{-}P}$ = 86.00 Hz. Whereas the *orto*- and *meta*-CH carbon atoms gave two doublets at 130.09 ppm (^{o}CH benzene ring, $^{o}J_{C\text{-}P}$ = 12.50 Hz) and at 133.83 ppm (^{m}CH benzene ring, $^{m}J_{C\text{-}P}$ = 10.20 Hz). The *para*-CH was finally found at 134.72 ppm and showed an insignificant CP coupling. The ^{31}P NMR spectrum evidenced only the singlet of the equivalent phosphorous atoms at 26.72 ppm, which is in accordance with the chemical shift reported for similar TPP derivatives. [36,37,50–52].

3.2. UV-Vis Analyses

In literature the UV-Vis spectra in water of four *bis*-triphenyl phosphonium bola-amphiphiles having C12, C16, C20 and C30 alkyl chains have been reported as acquired water and measuring the absorbance (Abs) in the range 250-320 nm [38], detecting three peaks of absorbance whose wavelengths have not been reported [38]. Here, the UV spectrum of BPPB was acquired in water, at room temperature, in the range 190-390 nm. Figure 7 shows the UV spectrum obtained.

 doi:10.20944/preprints202407.0891.v1

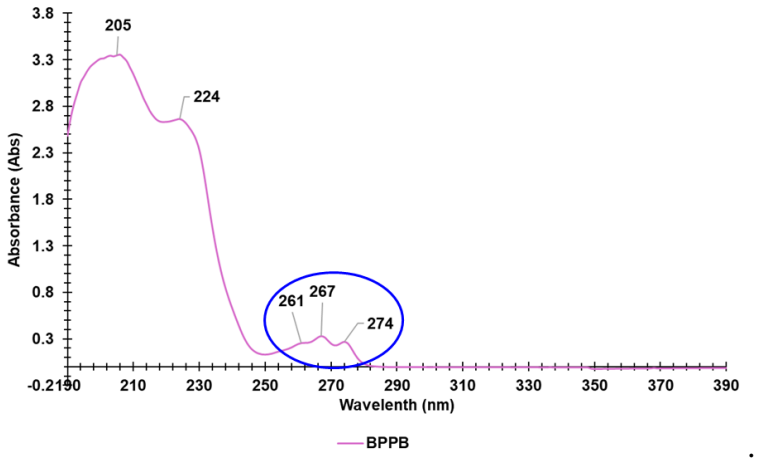

Figure 7. UV spectrum (water, 190-390 nm) of BPPB.

Using a BPPB solution at the same concentration reported by Ceccacci et al [38], but acquiring the spectrum in a larger range, it was possible for us to detect two very high peaks of absorbance under 250 nm (205 and 224 nm, Abs = 3.3 and 2.7), not reported previously, because of the too high cut-off adopted. The spectrum reported by Ceccacci et al, where three peaks of absorbance were detected in the range 250-290 nm (Abs of about 0.3), in our spectrum has been evidenced with the blue circle. In fact, by cutting and rescaling our spectrum as made by Ceccacci et al (Figure 8) a UV spectrum identical to that previously reported has been obtained [38].

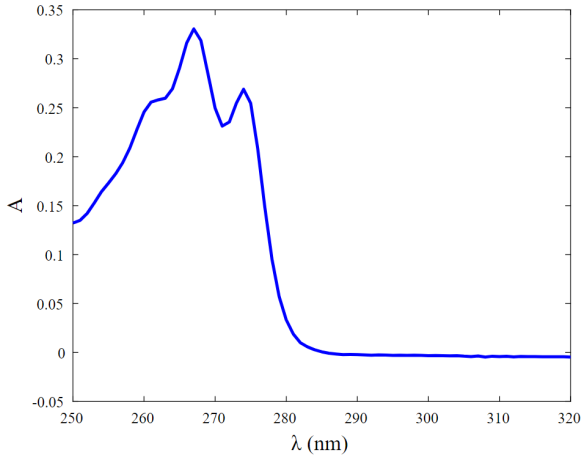

Figure 8. UV spectrum (water, 250-320 nm) of BPPB.

3.3. Potentiometric Titration of BPPB in Non-Aqueous Medium

The molecular weight (MW) and structure of BPPB, was further confirmed by titrating its phosphonium groups. By this method, the P^+ equivalents contained in an exactly weighted sample of PBBP were experimentally determined. Comparing the number of P^+ equivalents measures with that calculated according to the MW required by the formula of BPPB, we would have had validation of its mass and structure. In this regard, the emergence of non-aqueous titrations in the middle of the last century has enabled the possibility to determinate both weak acids and bases not measurable in aqueous media [53–55]. Especially, the titration of weak basic drugs with perchloric acid in glacial acetic acid medium is widely used. Titration in the acetic anhydride/acetic acid mixture enabled the direct non-aqueous titration of halide salts (mainly hydrochlorides) of organic bases and quaternary ammonium salts. By adding mercury (II) acetate reagent to the quaternary ammonium salts solution, stable mercury (II) halide complexes and free acetate ion (equivalent to the base) are formed, which can be titrated with perchloric acid [43,56]. On these considerations, we carried out the potentiometric

Preprints.org (www.preprints.org) | NOT PEER-REVIEWED | Posted: 11 July 2024 doi:10.20944/preprints202407.0891.v1

titration of BPPB in a mixture of anhydrous acetic acid (AcOH) and acetic anhydride (Ac_2O) 30:70 (v/v)), with 0.1 N $HClO_4$, performing a slightly modified procedure previously described by us for the volumetric titration of ammonium salts [40–42]. In brief, we reformed the method reported by Pifer and Wollish, who used this procedure to titrate quaternized ammonium salts [43], to examined BPPB. By plotting the measured mV values vs. the volumes of 0.1 N $HClO_4$ solution added, we gained the titration curves of BPPB (Figure 9) and the related first derivative (FD) curves.

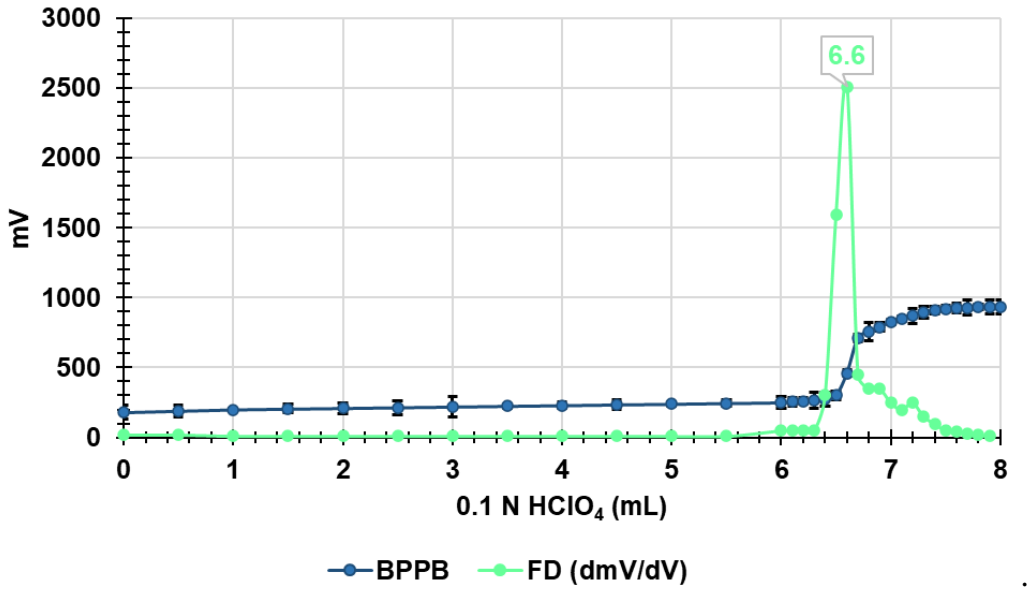

Figure 9. Potentiometric titration profiles of BPPB (blue line) and related first derivative curve (FD) (green line).

The maximum of the FD represents the titration endpoint, which allowed to find the volumes of titrating solution needed to titrate the phosphonium groups of our sample and then their P^+ equivalents. Table 1 reports the experimental details of titrations, the calculated P^+ equivalents for BPPB according to its molecular weight (MW = 852.70), the experimentally determined P^+ equivalents obtained by titrations, the experimental MW, the residuals and the percentage error (%).

Table 1. Data of potentimetric titration of BPPB.

Sample	Weight (mg)	* MW	* P^+ (mmol)	0.1 N $HClO_4$ (mL)	** P^+ (mmol)	** MW	*** Residuals	Error (%)
BPPB	280.0	852.7	0.6567	6.60	0.6600	848.5	4.2	0.5

* Calculated; ** experimental; *** refer to MW.

The experimental MW was perfectly in agreement with the calculated one, with an error (%) of 0.5%, thus further confirming the structure of BPPB.

3.4. Optical Microscopy Results

With the aim of using them, as mitochondria-targeted compounds in liposome formulations, Ceccacci et al prepared and investigated the colloidal behavior of four single-chain bola-amphiphiles compounds, having chains of different length linking two triphenyl phosphonium headgroups as BPPB [38]. The authors demonstrated that the studied bola-amphiphiles, upon dispersion in aqueous solution, in concentration higher than their critical aggregative concentration (CAC), were able to spontaneously self-assemble into vesicles, independently of the length of the hydrophobic spacer [38]. Particularly, the CAC for the compound having a C12 chain as BPPB was 3.6 mM and for DLS experiments, they prepared solutions 10 mM. The results evidenced the presence of 2 or more dimensional families. The authors assumed that particles with larger dimensions probably derived

 doi:10.20944/preprints202407.0891.v1

by the aggregation of smaller vesicles (about 20 nm) [38]. In this regard, before performing DLS analyses, we investigated the possible capability of BPPB to self-forming vesicular aggregate in water solution using optical microscopy. Briefly, we prepared a water dispersion 15.9 mM, which was clear under gentle heating, but opaqued on cooling, probably due to the formation of aggregates larger than those present in the clear solution, being the concentration 4.4-fold higher than the CAC of BPPB. The suspension was examined with a 40 × (Figure 10a) and 100 × (Figure 10b) objective observing spherical poly-dispersed vesicles.

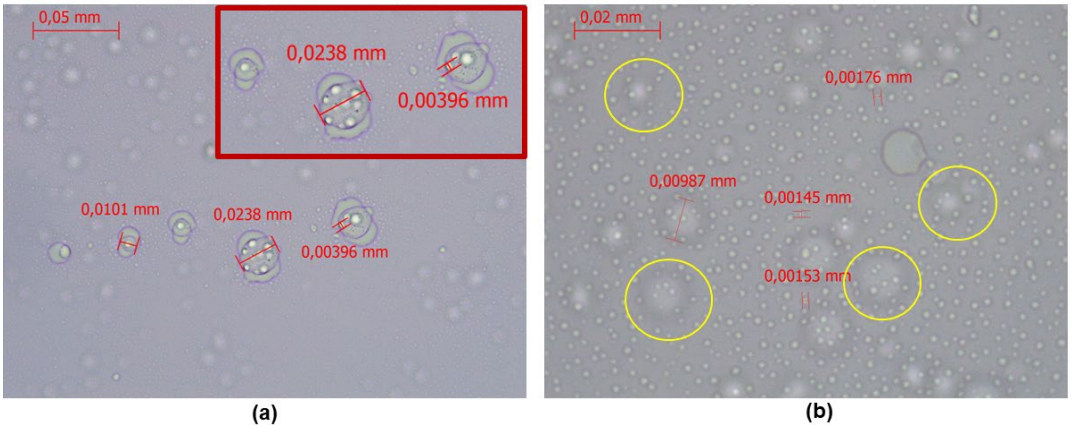

Figure 10. Vesicular aggregates of BPPB in water suspension as appeared with a 40 × objective (**a**), with a magnification in red square. Smaller vesicular aggregates of BPPB visible with the 100 × objective (**b**). In yellow circles larger aggregates have been evidenced.

Due to the high concentration of BPPB, very large aggregates (10-24 μm) were clearly visible using a 40 × objective, unequivocally formed by the aggregation of smaller ones (4 μm). Smaller spherical particles were also observable on background. Using the 100 × objective, it was possible to detect much smaller vesicles of 1.58 ± 0.13 μm on a background evidencing the larger aggregates previously observed in Figure 10a. We are aware that optical microscopy is not a precise method to evaluate the morphological and topographical characteristics of particles, because observations are strictly limited by the focus distance and light can be scattered differently in areas of different densities and geometries. Anyway, such technique has been used only to have preliminary results, which confirmed the reported capability of compound as BPPB to form spherical vesicles of different sizes, which sometimes coexist with aggregates of complex architecture [38]. An optical micrograph was acquired with a 4 × objective on solid BPPB, which showed an amorphous mass with evident traces of liquid, despite having been stored properly sealed with parafilm, thus confirming the high hygroscopicity of BPPB (Figure S1 in Supplementary Materials).

3.5. Particle Size, ζ-p and PDI of BPPB

The hydrodynamic size (diameter) (Z-AVE, nm) and polydispersity index (PDI) of BPPB vesicles were determined by DLS analysis to assess the dimensions of particles and how much their distribution could be uniform. To this end, BPPB solutions 5 mM filtered using a 0.22-micron filter were used. Additionally, ζ-p measurements were carried out on the same solution to determine their surface charge. Even if characterized by different sizes, preliminary investigations made using BPPB solutions 10 mM evidenced the presence of 2 dimensional families as previously reported [38]. Precisely, a small dimensional family made of particles of about 379 nm was detected, while the main family was made of very large particles of 1.6 μm (Figure S2 in Supplementary Materials), as those observed with the optical microscope (Figure 10b). As previously reported, these large particles should derive by the aggregation of smaller vesicles, probably promoted by the high concentration [38]. Upon 1:2 dilution, inverted results were obtained, and the main dimensional family was that with particle size of 379 nm (Figure S3), reproducing a process like that described by Ceccacci et al

 doi:10.20944/preprints202407.0891.v1

[38]. Upon filtration to disrupt residual aggregates, a main dimensional family made of small vesicles (< 50 nm) was observed as shown in Figure 11a, which reports a representative particles size distribution. Anyway, in other determinations, other small dimensional families including even smaller vesicles and larger aggregates were detected as shown in Figure S4. The variety of aggregates and vesicles found in DLS analysis is a sign of the well-known bolalipid's polymorphism [38]. Table 2 reports the average size (Z-AVE, nm) ± SD obtained by three measurements made of ten runs each one, as well as the mean value of PDI ± SD. Figure 11b shows a representative Zeta-potential distribution, while in Table 2 the mean ± SD of the values of ζ-p obtained by three measurements made of 12 runs each one has been included.

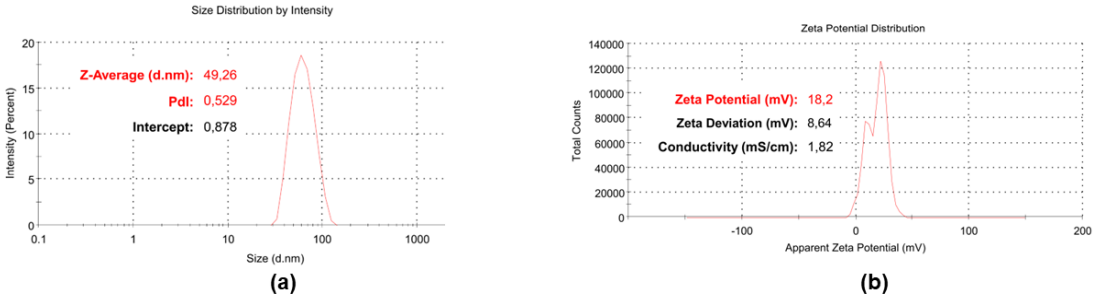

Figure 11. Representative images of the particle size distribution (nm) with DPI included of BPPB (**a**) and of its ζ-p (**b**).

Table 2. Results obtained from DLS analyses on BPPB 5 mM solution: particle size (Z-ave, nm), PDI and ζ-p.

Measure	PBBP * NPs
Z-Ave (nm)	45.28 ± 3.99
PDI	0.557 ± 0.03
ζ-p (mV)	+18.33 ± 0.98

Z-Ave = average hydrodynamic diameter; * solution 5 mM.

As evidenced by the DPI value (0.557) reported in Table 2, poly-dispersed nanosized vesicles of 45 nm were self-formed by BPPB in aqueous solution, with a positive ζ-p of +18 mV. As reported by Ceccacci et al., these findings could appear unusual, since generally, bola-amphiphiles with chain spacers of C8-C12 should form vesicles only when a double alkyl chain is present [57]. However, nanosized vesicles have been observed also for bola-amphiphiles with single chain, when a planar cationic headgroup, such as urocanic [58], quinolinium [59] and tri phenyl phosphonium moieties [38], as in our case, are present. This phenomenon occurs because self-assembly properties are strongly dependent on the complex interplay of non-covalent interactions (ionic, hydrophobic, π-π) inside the aggregate. In this regard, the π-π stacking between the 3 aromatic rings on polar heads of BPPB was crucial for the final aggregate morphology. Due to the morphology and size of BPPB and in sight of its possible future clinical administration as antibacterial agent, it must be considered that the size of nanoparticles strongly influences their distribution, cytotoxicity, and targeting ability [60–62]. Generally, biomedical applications require sizes lower than 200 nm, with an optimal of 100–200 nm [62] Due to the small dimension of its particles and hydro solubility, BPPB could be suitable for systemic administration. Additionally, very small particles as those of BPPB have a larger surface-area-to-volume ratio and are more effective and faster, do not tend to activate the lymphatic system and are removed from circulation slower [63]. BPPB proved positive ζ-p values (+18 mV), which was significantly different from that reported previously by Ceccacci et al [38]. Anyway, a positive surface charge is welcome for the development of highly effective nano-drugs. Based on the studies published so far, the internalization of positively charged NPs, is more efficient than that of neutral and anionic NPs [64–69]. Notably, it was found that after electrostatic interaction with anionic components of cell membrane as phospholipids, positively charged NPs can be internalized by

 doi:10.20944/preprints202407.0891.v1

several mechanisms, including pore formation, micropinocytosis, as well as clathrin- and dynamin-dependent endocytosis [65].

3.6. Antibacterial Properties

The antibacterial properties of BPPB were assessed first by determining its minimum inhibitory concentration values (MICs) on several clinical isolates of both Gram-positive and Gram-negative species, and then by performing 24-hour time-killing experiments on representative species.

3.6.1. In vitro Antibacterial Activity of BPPB: Determination of MIC Values (MICs)

Here, for the first time, the synthetic C12 *bis*-triphenyl phosphonium salt (BPPB) has been investigated as possible novel antibacterial therapeutic to treat severe human and/or animal infections sustained by MDR clinical isolated pathogens. In fact, while Wei et al, as well as Bin and Song reported the sterilizing action of this types of compounds on environmental bacteria not connected to difficult-to-treat human infections, no evaluation was ever carried out on MDR clinical strains, so far [34,35]. Both studies were conducted on saprophytic bacteria (TGB), sulfate-reducing bacteria (SRB) and iron bacteria (IB) of not clinical relevance and highlighter a sterilizing capacity of the compound at a high dosage of 20 mg/mL [34,35].

For MICs evaluation, a total of 50 strains (49 MDR isolates and a fully susceptible *E. coli* of clinical origin was exploited. Among enterococci, all strains were VRE, while staphylococci were all MRSA and MRSE. Three out of six *S. epidermidis* demonstrated resistance also to linezolid. Among Gram-negative bacteria, except for *E. coli* 224, all isolates considered presented a complex pattern of resistance, including cross resistances to carbapenems, colistin, CAZAVI and even the recently approved cefiderocol. We remind that colistin, or polymyxin E, is an older polycationic antibiotic often referred to as the "last-resort drug," and traditionally employed in the management of Gram-negative bacterial infections, particularly those sustained by *Enterobacteriaceae* that have developed resistance practically to all other antibiotics [70]. Unfortunately, starting from the year 2016, many Gram-negative bacteria have demonstrated to possess genes that confer resistance also to colistin, thus further reducing the available weapons to treat the infections they cause [70]. Furthermore, cefiderocol is a novel strategic catechol-substituted siderophore cephalosporin. It binds to the extracellular free iron and uses the bacterial active iron transport channels to penetrate in the periplasmic space of Gram-negative bacteria and kill them [71]. Nevertheless, cases of *in vivo* emerging cefiderocol resistance are increasingly being reported [72]. A variety of mechanisms of resistance have been reported, including β-lactamases (especially NDM, KPC and AmpC variants conferring resistance to ceftazidime/avibactam, OXA-427, and PER- and SHV-type ESBLs) production, porin mutations, and mutations affecting siderophore receptors, efflux pumps, and target (PBP-3) modifications [72]. On this background, it is of paramount importance and urgent to find novel compounds functioning on bacteria which have developed resistance also towards these last antibiotics. Moreover, *K. pneumoniae*, *K. aerogenes*, *E. cloacae*, *E. hormaechei* isolates and 4 out of 5 *E. coli* were β-lactamase producing bacteria, including metallo-β-lactamase NDM and VIM-1, against which no antibiotic is functioning [73,74]. Two out of four *P. aeruginosa* were isolated from cystic fibrosis patients, while two out of four were pyoverdine and pyocyanin-producing bacteria, which have been reported to be strains more tolerant to cationic antibiotics, due to a repulsive action exerted by such cationic pigments [75]. Despite this worrying and complex scenario of resistance of the clinical strains tested in this study, BPPB has demonstrated powerful effects on everyone, regardless of their resistance strategy. (Table 3 and Table 4).

 doi:10.20944/preprints202407.0891.v1

Table 3. MICs of BPPB against MDR clinical isolates of Gram-positive species obtained from experiments conducted at least in triplicate.

Strains	**BPPB** (852.7) [1]	**Reference antibiotics**
	MIC µg/mL	**MIC** µg/mL
E. faecalis 1 VRE	0.50	256 (V); 64 (T)
E. faecalis 79 VRE	0.50	256 (V); 128 (T)
E. faecalis 365 VRE	0.50	32 (V); 0.5 (T)
E. faecalis 425 VRE	0.50	32 (V); 1 (T)
E. faecium 152 VRE	0.25	128 (V); 64 (T)
E. faecium 182 VRE	0.25	64 (V); 1 (T)
E. faecium 364 VRE	0.50	32 (V); 0.5 (T)
E. faecium 479 VRE	0.50	64 (V); 1 (T)
S. aureus A MRSA	0.25	256 (O)
S. aureus B MRSA	0.25	512 (O)
S. aureus D MSSA	0.25	1 (O)
S. aureus F MSSA	0.50	0.5 (O)
S. aureus 17 MRSA	0.25	256 (O)
S. aureus 18 MRSA	0.25	512 (O)
S. aureus 187 MRSA	0.50	256 (O)
S. aureus 195 MRSA	0.25	256 (O)
S. epidermidis 195 MRSE	0.25	256 (O)
S. epidermidis 2 MRSE	0.25	128 (O)
S. epidermidis 22 MRSE	0.25	128 (O)
S. epidermidis 171 MRSE *	0.25	256 (O)
S. epidermidis 178 MRSE *	0.25	64 (O)
S. epidermidis 181 MRSE *	0.50	256 (O)

[1] MW of compounds; VRE = vancomycin-resistant enterococci; MRSA = methicillin resistant *S. aureus*; MRSE = methicillin resistant *S. epidermidis*; * denotes also linezolid resistance; V= vancomycin, T= teicoplanin, O= oxacillin.

Table 4. MICs of BPPB against MDR clinical isolates of Gram-negative species obtained from experiments conducted at least in triplicate.

Strains	**BPPB** (852.7) [1]	**Reference antibiotics**
	MIC µg/mL	**MIC** µg/mL
P. aeruginosa 1V °,*	32	16 (M)
P. aeruginosa 2V °,*	16	16 (M)
P. aeruginosa 259 °,*,**	32	4 (M)
P. aeruginosa 265 MDR ***	32	16 (M)
A. baumannii 257 *	8	16 (M)
A. baumannii 279 *	8	16 (M)
A. baumannii 283 *	4	8 (M)
A. baumannii 236 *	8	16 (M)
A. baumannii 406 *	8	8 (M)
S. maltophylia 280	1	0.5 (TMP-SMX)
S. maltophylia 384 [R TMP-SMX]	4	32 (TMP-SMX)
S. maltophylia 390	2	1 (TMP-SMX)
S. maltophylia 39	2	0.5 (TMP-SMX)
S. maltophylia 392	2	0.5 (TMP-SMX)
K. pneumoniae 376 *,[KPC]	16	32 (M)
K. pneumoniae 377 *,[KPC]	16	16 (M)
K. pneumoniae 488 *,[KPC]	16	32 (M)
K. pneumoniae 490 *,[KPC],***	16	32 (M)

 doi:10.20944/preprints202407.0891.v1

K. pneumoniae 540 *,VIM, RC	16	32 (M)
K. aerogenes 500 *,KPC	16	64 (M)
E. coli 224 S	1	0. 03 (M)
E. coli 462 *,NDM	2	32 (M)
E. coli 477 *,KPC	1	16 (M)
E. coli 539 *,NDM, RC	2	32 (M)
E. coli 525 *,VIM	16	32 (M)
E. cloacae 517 *,VIM	16	8 (M)
E. cloacae 527 *,VIM	32	32 (M)
E. hormaechei 544 *,VIM, RC	32	32 (M)

[1] MW of compounds; ° from patients with cystic fibrosis; * resistant to carbapenems; ** ceftazidime-avibactam (CAZAVI) resistant; *** colistin resistant; KPC = *K. pneumoniae* carbapenemase-producing bacteria; VIM = VIM-1 metallo-β-lactamase-producing *K. pneumoniae*; RC = cefiderocol-resistant; NDM = New Delhi metallo-β-lactamase-producing *E. coli*; S = fully susceptible strain; TMP-SMX = trimethoprim-sulfamethoxazole; R TMP-SMX = resistance to trimethoprim and sulfamethoxazole.

Very low MICs, in the range 0.25-0.50 μg/mL (0.29-0.59 μM), were observed on all Gram-positive VRE, MRSA and MRSE isolates here considered. These results evidence the high potentialities of BPPB to be developed as a new effective treatment for severe infections sustained by Gram-positive pathogens included in the ESKAPE group [76]. These are worrying Gram-positive and Gram-negative MDR pathogens, which have developed the capability to "escape" the traditional antibiotics, especially in the hospital setting Particularly, VRE enterococcal species are MDR bacteria that in addition to resistance to vancomycin, have already developed a variety of mechanisms of resistance to several other antibiotics like aminoglycosides, β-lactams, tetracyclines, and quinolones. Additionally, they can produce β-lactamases, and have decreased cellular permeability, thus being the cause of severe hospital-acquired infections [77]. VRE are reported as the responsible number one for central line-associated bloodstream infections (CLABSI), number three for catheter-associated urinary tract infection (CAUTI), number eleven for ventilator-associated pneumonia (VAP) and number two for surgical site infections (SSI) [78]. Therefore, being BPPB active against these bacteria at very low dosage (0.25-0.5 μg/mL) and considering the low cytotoxicity demonstrated in vitro against eukaryotic cells (see later in the paper) could represent the urgently required pharmacological tool, necessary to limit infections by VRE, categorized as a "serious threat" by Centers for Disease Control (CDC) and Prevention [78]. Even more relevant is the effectiveness demonstrated by BPPB against staphylococci and especially against MRSA, which ranks first in the USA, in nosocomial infections, antibiotic-resistant pathogenic diseases, central line-associated bacteremia, and hospital-associated endocarditis [79,80]. Notably, MRSA is the first most common cause of community-acquired endocarditis in North America [81]. Very common in hospitals, prisons, and nursing homes, where immunocompromised patients, and people with open wounds and/or invasive devices such as catheters, are at greater risk of hospital-acquired infections, MRSA represents a global health threat and a clear 'One Health' problem. Moreover, MRSA can spread between and impact the environment, animals, and several human sectors [82].

Against MRSA, vancomycin is currently successful in approximately 49% of cases only, and its use is complicated by its inconvenient route of administration [83].

Unfortunately, several strains of MRSA have shown resistance even to vancomycin and teicoplanin from the late 1990s [84]. Oxazolidinones such as linezolid, available from 1990s, was initially beneficial to address resistance to vancomycin, but cases of bacteria tolerant also towards linezolid have been reported from 2001 [85].

Anyway, for surgical site infections (SSIs) by MRSA [86] and for MRSA colonization in nonsurgical wounds such as traumatic wounds, burns, and chronic ulcers (i.e., the diabetic ulcer, pressure ulcer, arterial insufficiency ulcer, and venous ulcer), no conclusive evidence has been found about the best antibiotic regimen to be used [87]. In this alarming scenario, made of missing epidemiologic evidence, a plethora of uncertainties due to the interindividual responses of patients to existing antibiotics, and of a decreasing efficacy of available drugs, the development of new

 doi:10.20944/preprints202407.0891.v1

curative options against MRSA infections is urgent. Therefore, another merit of the present study consists of having identified in BPPB, a potential new and strong antibacterial agent against MRSA, more active than the most of quaternary phosphonium salts developed so far, as discussed in the following section. Higher MIC values were found on Gram-negative bacteria, but overall low (1-32 μg/mL (1.2-37.5 μM)), if we consider the very complex resistance model of strains used. Their distinctive structure makes them more difficult to be inhibited, than Gram-positive bacteria, thus being responsible of even high morbidity and lethal infections worldwide [88,89]. The highest MICs of 16-32 μg/mL were observed on MDR *K. pneumoniae* and *K. aerogenes* (16 μg/mL), *P. aeruginosa* (16-32 μg/mL), *E. cloacae* (16-32 μg/mL) and *E. hormaechei* (32 μg/mL) isolates. Lower MICs (4-8 μg/mL) were instead observed on MDR *A. baumannii* isolates, while MICs even lower up to 1 μg/mL were found towards MDR isolates of *E. coli* and *S. maltophilia* regardless their broad resistance and/or their resistance to carbapenems. Isolates of genera *Klebsiella, Escherichia,* and *Enterobacter* make part of the Gram-negative *Enterobacteriaceae* family. [90]. Today, *K. pneumoniae* is the most common cause of hospital-acquired pneumonia in the United States, and the organism accounts for 3% to 8% of all nosocomial bacterial infections. It is noteworthy that, the capability of *K. pneumoniae* to hydrolyze a very broad spectrum of β-lactam substrates, including penicillin, cephalosporins, monobactams and carbapenems, is weakly inhibited by traditional β-lactam inhibitors (i.e. clavulanic acid and tazobactam), and only the novel β-lactamase inhibitors (i.e. diazabicyclooctanes and boronates) are successful in contrasting isolates of this specie [73,74,91,92]. *K. aerogenes*, and other *Enterobacter* species such as *E. cloacae* and *E. hormaechei* are responsible of bloodstream infections (BSI). BSI sustained by *K. aerogenes,* and *E. cloacae* often presents poor clinical outcomes (death before discharge, recurrent BSI, and/or BSI complication), which are higher for *K. aerogenes* than *E. cloacae* [90]. In this regard, pan-genome analysis revealed genes unique to *K. aerogenes* isolates, including putative virulence genes involved in iron acquisition, fimbriae/pili/flagella production, and metal homeostasis [90]. Anyway, antibiotic resistance was largely found also in *E. cloacae*. Isolates of genera *Pseudomonas, Acinetobacter,* and *Stenotrophomonas* make part of the Gram-negative non-fermenting bacteria. *P. aeruginosa* is commonly isolated from patients, affected by both monomicrobial and polymicrobial infections [93]. The spectrum of infection caused by *P. aeruginosa* is wide, and involvement of multiple organ systems is not uncommon [93]. To have available drugs active against these bacteria has become a significant problem and, to some extent, spurs the development of novel antimicrobial agents. Not less important, *Acinetobacter* species, mainly including *A. baumannii*, have developed resistance to multiple agents thus representing a common thread, being their infections associated with substantial morbidity and mortality [93]. *S. maltophilia* is intrinsically drug-resistant to an array of different antibiotics and uses a broad arsenal to protect itself against antimicrobials. Surveillance studies have recorded a worrying increase in drug resistance for *S. maltophilia*, prompting new strategies to be developed against this opportunist bacteria [94]. Although infection control and antimicrobial stewardship are important tools in combating the development and spread of infections caused by these bacteria, novel appropriate antimicrobial therapies are urgently needed. In this scenario, thanks to this study, towards all these bacteria, intractable with currently available antibiotics and responsible for serious life-threatening infections, it will be possible to hypothesize a future use of BPPB developed here.

An Overview of Previous Achievements by Using Antibacterial Phosphonium Salts

Ermolaev et al. synthesized a series of 20 sterically hindered quaternary phosphonium salts having one cationic head, which were tested on selected Gram-positive and Gram-negative bacteria and fungi, including among others strains of *E. faecalis*, MRSA, *E. coli* and *P. aeruginosa*, considered also by us [1]. According to the MICs reported by authors for these isolates, when tested on several MRSA and VRE *E. faecalis* strains, BPPB demonstrated to be more potent than all compounds developed and tested by Ermolaev [1]. Additionally, when ciprofloxacin was tested by authors, it demonstrated MICs higher than those of BPPB by 1.8-500 times against MRSA, and by 7.8-15.6 times against an *E. faecalis* isolate whose pattern of resistance has not been clearly reported [1]. Pugachev and colleagues synthesized 13 pyridoxine-based phosphonium salts and tested *in vitro* their

 doi:10.20944/preprints202407.0891.v1

antibacterial effects on Gram-positive isolates of staphylococcal genus and on strains of *K. pneumoniae* and *Proteus* spp genus, as representative isolates of Gram-negative species [30]. No compound including vancomycin, that authors tested on their bacteria as a reference antibiotic, was active on Gram-negative bacteria (MICs > 1000 μg/mL), while the best performant molecule (compound 20) demonstrated MICs = 5 μg/mL against both *S. aureus* and *S. epidermidis*, by cell penetration and interaction with genomic and plasmid DNA [30]. On these results, BPPB was 10-20-fold more potent than compound 20 developed by Pugachev and colleague against MRSA and MRSE [30]. When vancomycin was used by authors on *S. aureus* and *S. epidermidis* of their study, it demonstrated MICs 5-10 times higher than those displayed by BPPB against MRSA and MRSE [30]. The same year, phosphonium salts with two cationic heads like BPPB, were synthesized by Pugachev et al. Particularly, the authors produced 23 novel *bis*-phosphonium salts based on pyridoxine and their antibacterial activities were evaluated *in vitro*. As in their previous study, despite the presence of two cationic heads, all compounds were inactive against Gram-negative bacteria, including a *K. pneumoniae* isolate (MICs > 1000 μg/mL). On the contrary, BPPB displayed low MICs = 16 μg/mL, on all *K. pneumoniae* isolates tested, regardless of their resistance to carbapenems, their capability to produce of KPC and/or VIM-1 β-lactamase, and/or their resistance to cefiderocol. The compounds developed by Pugachev et al exhibited structure-dependent activity against Gram-positive isolates [36]. Anyway, in the best cases (compound 14a and 10a in the study), MICs against *S. aureus* and *S. epidermidis* with not specified resistance were 1-1.25 μg/mL, thus establishing that BPPB was 2-5-fold more potent than 10a and 14a, regardless the MDR MRSA and MRSE strains used by us [36]. In the past, Cieniecka-Roslonkiewicz and co-workers synthesized 21 alkyl phosphonium salts and essayed them against a selection of Gram-positive and Gram-negative ATCC bacteria. From the reported results, the best performant compounds prepared by the authors were 4-8-fold less active than BPPB when used on MRSE, 4.6-9.2 less potent than BPPB when tested against MRSA, and 4.6-9.2 less potent than BPPB when proved against VRE *E. faecium* [31]. Additionally, when benzalkonium chloride was used by authors on ATCC strains of *S. epidermidis*, *S. aureus*, and *E. faecium*, MICs 2.8-5.6-, 5.6-11.2-, and 11.2-22.4-times higher than those shown by BPPB against MDR isolates used by us were detected [31]. More recently, Lei et al. synthesized two mono- and one *bis*-quaternary phosphonium tosylate compounds with different lengths of oligo-(ethylene glycol) (OEG) chains and TPP^+ moieties as antibacterial group [37]. The aim of authors was to find new antibacterial compounds with less toxicity with respect to TPP-based smaller molecules previously reported. As expected, when synthesized compounds were essayed on *S. aureus* and *E. coli*, the *bis*-quaternary phosphonium salt was remarkably more active than mono ones, but the lowest MICs recorded were 1.5 mg/mL on *S. aureus* and 3.1 mg/mL on *E. coli*. Collectively, although when administered at concentrations up to 2.5 mg/mL (only 1.7 × MIC) to eukaryotic cells, viable cells were almost the 80% respect to control after 3 days, the doses necessary to inhibit *S. aureus* and *E. coli* ATCC strains were 3000-6000-fold and 1550-3100-fold higher respectively, than those of BPPB, which were necessary to inhibit MRSA and MDR *E. coli* isolates. BPPB was also more effective than a phosphonium salt recently reported by us (compound 1 in the study) and tested on Gram-positive and Gram-negative isolates with complex pattern of resistance like that of strains used in this study [12]. Completely inactive against Gram-negative species, 1 was 8-32-times less active than BPPB on staphylococci and 16-64-times on enterococci [12]. Very recently, Nunes and co-workers, synthesized seven C6-C18 alkyl triphenyl phosphonium salts among a library of 49 QASs and QPSs, and evaluated their antibacterial effect on antibiotic-sensitive and antibiotic-resistant *S. aureus* [89]. Collectively, salts with C12-C14 alkyl chains were the best performant antibacterials, being phosphonium salts significantly more efficient than ammonium compounds. When tested on antibiotic-resistant *S. aureus*, C14 alkyl triphenyl phosphonium salt (1e) displayed MICs = 1-2 μg/mL, thus establishing that BPPB was more potent by 2-8 times. On these resistant strains, erythromycin, tetracycline and ciprofloxacin, tested by authors for comparison, displayed MICs 512-1024-fold, 256-512-fold, and 256-512-fold higher than those demonstrated by BPPB on eight MDR MRSA [89]. Also, when eight new chiral quaternary phosphonium salts (CQPSs) comprising (1R,2S,5R)-(–)-menthyl or (1S,2R,5S)-(+)-menthyl groups, were tested by Arkhipova and colleagues on Gram-positive MRSA-1 and MRSA-2 strains, sensitive

 doi:10.20944/preprints202407.0891.v1

E. faecalis; as well as on *E. coli* and *P. aeruginosa,* as Gram-negative pathogenic bacteria, they were all inactive against the latter species. Better activity was observed against MRSA and *E. faecalis*, but the best performant compound was 15.6-31-fold less active than BPPB when was examined against MRSA and VRE *E. faecalis* [50]. From literature data about the antibacterial performance of previously reported phosphonium salts, it was possible to compare the antibacterial properties of BPPB with those of previously reported similar compounds only concerning *E. coli, P. aeruginosa*, and/or *K. pneumoniae,* because the other clinically relevant species assayed in this study, have not been considered by other authors which handled phosphonium salts. BPPB demonstrated antibacterial effects against MDR *E. coli* and *P. aeruginosa*, comparable or higher than those showed by sterically hindered quaternary phosphonium salts having one cationic head on sensitive strains of the same genus [1]. Differently from our BPPB, all the 21 alkyl phosphonium salts developed by Cieniecka-Rosłonkiewicz were not active against *P. aeruginosa*, while the best performant compound was 1.25-2.50-fold less active than BPPB on an isolate of *E. coli* with not specified pattern of resistance [31]. When benzalkonium chloride was used on *E. coli* and *P. aeruginosa* tested in the study by Cieniecka-Rosłonkiewicz, it demonstrated MICs 1.4-2.8-times and 5.5-11-times higher than those displayed by BPPB against isolates of the same genus but with complex resistance profiles [31]. A very recent interesting study by Summers and co-workers reported the synthesis, characterization and antibacterial properties of 59 quaternary phosphonium compounds (QPCs) including mono-QPCs, bis-QPCs, tris-QPCs, and tetra-QPCs, bearing 1 to 4 C8-C18 hydrocarbon tails [95]. Their antibacterial activity was essayed against two strains of MRSA, one MSSA, one *E. faecalis*, one *E. coli* and one *P. aeruginosa*, evidencing MICs in the ranges 0.5-125 μM on MRSA, 0.5-16 μM on MSSA, 2->250 μM on *E. faecalis*, 2->250 on *E. coli* and 4->250 on *P. aeruginosa.* On these results, BPPB was more potent than all compounds reported in the study on MRSA, *E. faecalis*, and *E. coli* [95]. Additionally, although 13 of compounds reported by Summers et al were more active than BPPB on *P. aeruginosa* used in their study, *P. aeruginosa* isolates used by us presented a much more complex pattern of resistance [95].

3.6.2. Time-Killing Curves

To assess whether BPPB was bactericidal or bacteriostatic, time-kill experiments were performed at concentrations equal to 4 × MIC on strains of MRSA and *E. coli*. Particularly, isolates 17, 18, 187 and 195 of MRSA and strains 477, 525 and 539 of *E. coli* were used. As depicted in Figure 12, reporting the most representative curve obtained for MRSA strain 18 and *E. coli* 539, BPPB showed bacteriostatic effects against both species, since a decrease of < 3 log in the original cell number was evident after 6 h of exposure. During the next hours up to 24, a slight increase and regrowth occurred.

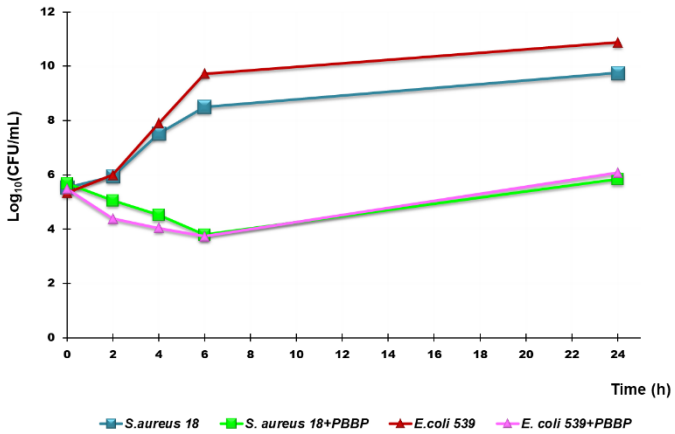

Figure 12. Time-killing curves performed with PBBP (at concentrations equal to 4 x MIC) on *S. aureus* 18 and *E. coli* 539.

 doi:10.20944/preprints202407.0891.v1

A series of quaternary phosphonium (QP) N-chloramine molecules, covalently combining a N-chloramine and a QP moiety via aliphatic chains made of different methylene units were synthesized using multi-step chemical reactions [96]. Compared with a quaternary ammonium salt synthesized by authors as reference compound, QP compounds displayed significantly higher antibacterial effects and were biocidal depending on the time of exposure [96]. While the QP N-chloramine compounds with a C3-C12 chains as linkers (compounds 3-6), all demonstrated high biocidal efficacy after 10 minutes of contact causing a 6.22 and 7.30 CFU log reduction in the initial inoculum of *E. coli* and *S. aureus* respectively, compound 6 bearing a C12 chain was bactericidal also after only 5 minutes contact [96]. This suggests that a future chemical modification of PBBP by inserting N-chloramine residues could be a strategy to convert the bacteriostatic effects observed for PBBP in bactericidal ones.

3.7. Cytotoxicity Experiments on Eukaryotic Cells

The assessment of cytotoxicity towards eukaryotic cells is essential to predict the possible development of new compounds as antimicrobial agents suitable for clinical application. As reported, the cytotoxicity of QPSs could depend on different their physicochemical characteristics, such as the length of alkyl chains, the presence of aromatic ring(s), on which the P^+ cation can delocalize, thus conferring the molecules a softer charge [38], the type of anion, the possible colloidal properties, and the capability or not to form nano aggregates [89]. Additionally, QPSs cytotoxicity could only depend on the specific cell type under investigation [89]. Concerning this, bacteria as well as cancer cells present differences from mammalian cells. The presence on the bacterial surface of lipids with a net anionic charge in place of zwitterionic lipids neutral at physiological pH present in that of mammalian cells translates into a significant disparity in membrane electrostatic charges thus resulting in the targeted tropism of cationic antimicrobial agents toward negatively charged bacteria [27]. Additionally, cholesterol present in mammalian cell membranes and missing in those of bacteria could provide selective protection to eukaryotic cells thus reducing the possible cytotoxicity of a novel antibacterial compound upon exposure. Anyway, depending on the concentration, time of exposure and the abovementioned structural properties of QPSs, cytotoxicity may still manifest in mammalian cells [89]. In this study, the cytotoxicity profile of BPPB, was assessed in both human liver cells (HepG2) cells as in our previous work [12]and in transformed African green monkey kidney fibroblast cells (Cos-7). HepG2 cells are commonly employed in drug metabolism and hepatotoxicity studies [97–99], while Cos-7 are commonly used in toxicology research and gene-transfection experiments. Since HepG2 cells exhibit a non-tumorigenic nature, display high proliferation rates, and possess an epithelial-like morphology while retaining many differentiated hepatic functions [100,101], they represent a useful model for evaluating the cytotoxic effects of novel compounds. A sufficiently high value of the selectivity index (SI) is an essential requirement to render a new molecule worthy of consideration for further studies and future development as new therapeutic agent. The SI value is given by the equation Eq. (1) and provides a measure of the selectivity of the antimicrobial agent for bacteria.

$$SI = IC_{50}/MIC \quad (1)$$

In Eq. (1), IC_{50} is the concentration of a compound capable to reduce viable cells by 50%, while MIC is the minimum inhibitory concentrations determined for a specific isolate. To obtain the SI values of PBBP, we carried out dose dependent experiments, using the MTT cells proliferation tests. Additionally, we evaluated the cytotoxicity of PBBP also carrying out the lactate dehydrogenase (LHD) cytotoxicity essay which measures the LDH activity as an indicator of cell death. The results from the MTT test were used to calculate the IC_{50} values on both cell lines and the obtained IC_{50} and the MICs which were observed most frequently for each bacterial species considered (Table 3 and 4) were then used to calculate the SI values.

3.7.1. Assessment of the PBBP Concentration-Dependent Effects on Cos-7 and HepG2 Cells by MTT and LDH Essays

 doi:10.20944/preprints202407.0891.v1

Both cell lines were exposed for 24 hours to different concentrations of BPPB (0.5-100 µg/mL (0.0 µg/mL was the control) on the base of the observed MICs. Growth inhibition/death were determined by the MTT test, while cell cytotoxicity was determined by LDH assay. Results have been reported as bar graphs in Figure 13 and as dispersion graphs in Figures S5 and S6 in Supplementary Materials.

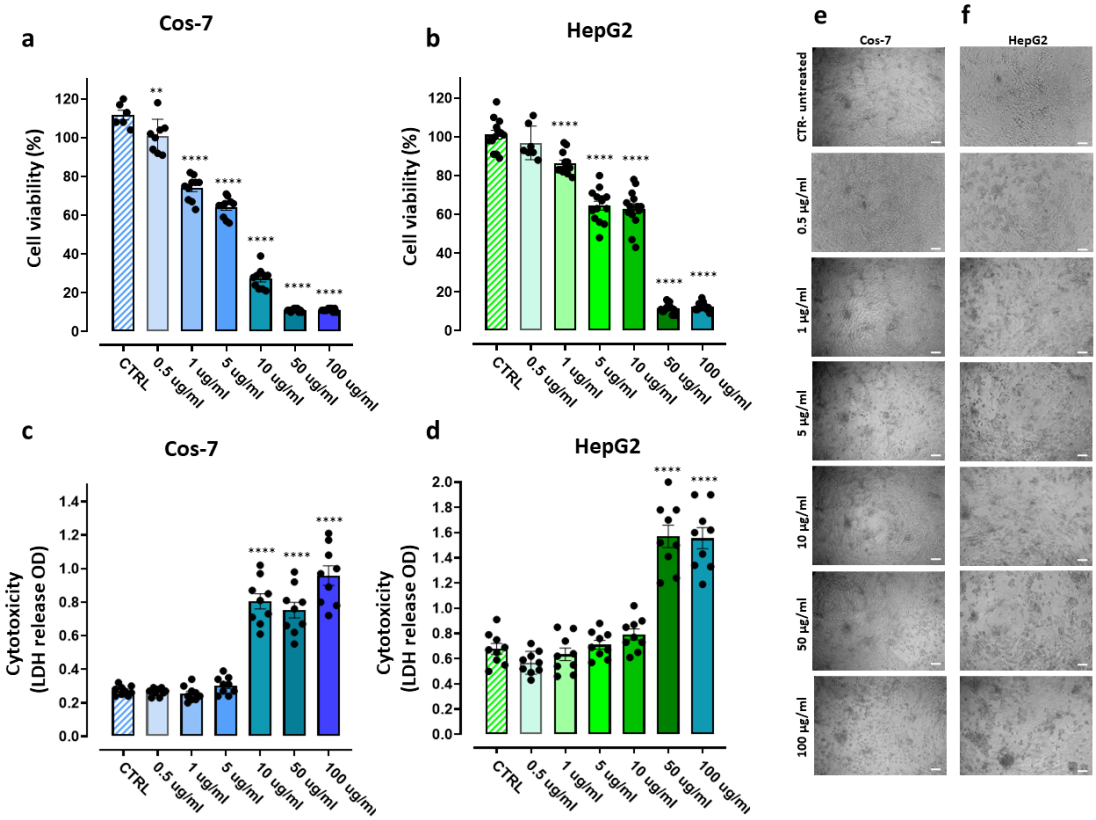

Figure 13. *Growth inhibition and cytotoxic effects of PBBP on Cos-7 and HepG2 cells.* Cos-7 and HepG2 cells were seeded on 96-multiwell plates and treated for 24h with different concentrations (0.5-100 µg/mL) of bis-phosphonium bromide. Growth inhibition was determined by MTT assay (**a-b**). The bar graph shows the cell viability (%) of Cos-7 (**a**) and HepG2 (**b**) cells untreated (CTRL), and after exposure to increasing concentrations (0.5-100 µg mL^{-1}) of PBBP for 24h. Data are expressed as the mean ± S.E.M. of the survival percentage obtained from n = 6-14 independent experiments run in triplicate. Significance is indicated as ** $p<0.005$ and **** $p<0.0001$ vs. CTRL (one-way ANOVA followed by Tukey's multi-comparisons test). Cell cytotoxicity was determined by LDH assay (**c-d**). The bar graph shows the quantification of cell damage (expressed as optical density units of absorbance) of Cos-7 (**c**) and HepG2 (**d**) cells untreated (CTRL), and after exposure to increasing concentrations (0.5-100 µg mL^{-1}) of bis-phosphonium bromide for 24h. Data are expressed as the mean ± S.E.M. of the cell cytotoxicity (OD units recorded, in kinetic mode, after 10 minutes of LDH reaction), obtained from n = 6-14 independent experiments run in triplicate. Significance is indicated as **** $p< 0.0001$ vs. CTRL (one-way ANOVA followed by Tukey's multi-comparisons test). (**e-f**) Representative phase contrast images of Cos-7 (**e**) and HepG2 (**f**) cells acquired in untreated conditions or after exposure to increasing concentrations (0.5-100 µg mL^{-1}) of bis-phosphonium bromide for 24h.

Particularly, in the case of the MTT test (Figure 13a and 13b), bar graphs show the cell viability (%) of Cos-7 (**a**) and HepG2 (**b**) cells untreated (CTRL), and after exposure to the increasing concentrations of PBBP for 24h, while in Figure 13c and 13d, we have plotted the quantification of cell damage (expressed as optical density (OD) units of absorbance)) of Cos-7 (**c**) and HepG2 (**d**) cells untreated (CTRL), and after exposure to increasing concentrations of PBBP for 24h. Moreover, representative phase contrast images of Cos-7 (**e**) and HepG2 (**f**) cells acquired in untreated conditions or after exposure to increasing concentrations PBBP for 24h have been reported.

 doi:10.20944/preprints202407.0891.v1

According to the results shown in Figures 13a and 13b, in the MTT test, BPPB demonstrated concentration-dependent effects towards both cell lines. Anyway, for concentrations = 10 μg/mL, while on HepG2 cells, BPPB exerted effects like those observed at 5 μg/mL and cell viability was higher than 50% and similar (64.5% vs. 62.9%) at both concentrations, cell viability of Cos-7 decreased under 30% (27.45%) respect that observed at 5 μg/mL (64.2%). Collectively, the MTT test evidenced that cell viability was affected by BPPB exposure in a major extent in Cos-7 cells than in HepG2 ones, and a safety profile was detected at concentrations ≤ 5 μg/mL towards Cos-7 and ≤ 10 μg/mL towards HepG2 cells, which is, however, a scenario more satisfactory than that reported by Nunes et al, for the best performing antibacterial compounds they recently synthesized [89]. From LDH test results (Figure 13b and 13c) a slightly different scenario was evidenced in which, while a dose-dependent effect was observed at concentrations ≥ 10 μg/mL on Cos-7 cells and similar cell damage was observed for concentrations ≤ 5 μg/mL, on HepG2 cells a dose-dependent effect was observed at concentrations ≤ 10 μg/mL and similar cell damage was observed for concentrations ≥ 50 μg/mL. Nonetheless, as observed in MTT test, for concentrations = 10 μg/mL, while on HepG2 cells, BPPB caused damage like that observed at 5 μg/mL and the optical density due to LDH release was similar (OD = 0.71 vs. 0.79) at both concentrations, that measured on Cos-7 cells remarkably increased (OD = 0.80) respect that observed at 5 μg/mL (OD = 0.30), thus evidencing remarkably higher cell damage. Collectively, also the LDH test evidenced that a safety profile exists at concentrations ≤ 5 μg/mL towards Cos-7 and ≤ 10 μg/mL towards HepG2 cells.

3.7.2. IC_{50} and Selectivity Indices

For a more precise evaluation of the effects of BPPB on eukaryotic cells here considered, we calculated the IC_{50} OF BPPB on both cell lines using GraphPad Prism software and fitting data with non-linear regression models. Particularly, we plotted the Log_{10} of the concentrations vs. the values of cell viability observed and the fitting nonlinear models were achieved (Figure S7 in Supplementary Materials). The calculated IC_{50} values were 5.76 ± 0.95 μg/mL and 11.31 ± 1.54 μg/mL on Cos-7 and HepG2 cells respectively, thus confirming the significantly dissimilar cytotoxicity of BPPB on the different cells, being Cos-7 the cells less tolerant to PBBP and confirming the previously reported assertion that the toxicity of a new compound strongly depends on the type of cell line used [89]. In this regard, considering that Cos-7 cells are derived from a non-human source, results obtained using Cos-7 cells may not be directly applicable to human biology. So, the lower toxicity of PBBP found toward human hepatic cells with respect to monkey kidney ones and not the contrary is a very promising result, which could pave the way for the future clinical development of PBBP and its possible derivatives. Additionally, since it is believed that the HepG2 cell line retains most of the metabolic functions of normal hepatocytes; and it is commonly used to study the toxic effects of heavy metals, nanoparticles, and drugs in vitro [102], we retained more reliable cytotoxicity results obtained on HepG2 than those obtained on Cos-7 cells. Anyway, to assess the bacterial species against which PBBP could be though as a new promising therapeutic treatment, using Eq. (1), the values of IC_{50} from the MTT test, and the MICs observed with most frequency for all bacterial species reported in Tables 3 and 4, the SIs of BPPB were calculated for both cell lines. The results have been included in the following Table 5 for Gram-positive isolates and Table 6 for Gram-negative ones.

Table 5. MICs of BPPB observed with most frequency against MDR clinical isolated of Gram-positive species and selectivity indices (SIs) towards Cos-7 and HepG2 cells.

Strains	**BPPB** (852.7) [1]	**Cos-7**	**HepG2**
	MIC (μg/mL)	**SI**	**SI**
E. faecalis	0.50	11	23
E. faecium	0.25-0.50	11-22.	23-46
S. aureus	0.25	22	46
S. epidermidis	0.25	22	46

[1] MW of BPPB; SI = IC_{50}/MICs.

 doi:10.20944/preprints202407.0891.v1

Table 6. MICs of BPPB observed with most frequency against MDR clinical isolated of Gram-negative species and selectivity indices (SIs) towards Cos-7 and HepG2 cells.

Strains	**BPPB** (852.7) [1]	**Cos-7**	**HepG2**
	MIC (μg/mL)	**SI**	**SI**
P. aeruginosa	32	0.2	0.4
A. baumannii	8	0.7	1.4
S. maltophylia	2	2.8	5.6
K. pneumoniae	16	0.4	0.7
K. aerogenes	16	0.4	0.7
E. coli	1-2	5.5-2.8	11.3-5.6
E. cloacae	16-32	0.4-0.2	0.7-0.4
E. hormaechei	32	0.2	0.4

[1] MW of PBBP; SI = IC_{50}/MICs.

For prospective antimycobacterial drugs, it has been proposed that the selectivity index should be greater than ten before they are considered for further development [103]. Accordingly, and according to findings reported in Tables 5 and 6, and considering the most reliable results, those achieved on HepG2 cells, PBBP could be considered very promising as an effective agent against the most worrying MDR bacterial strains of Gram-positive species tested here and *E. coli*, thus providing valuable insights for the rational design of other PBBP like derivatives with enlarged SI values.

4. Conclusions

In this study, a new potent antibacterial agent possessing bacteriostatic effects against MDR clinical isolates of Gram-positive and Gran-negative species including ESKAPE bacteria has been developed. By performing a low-cost one-step reaction, a *bis*-triphenyl phosphonium dibromide salt bearing a C12 alkyl chain as a linker between the two cationic heads (BPPB) was prepared and fully characterized. Known for its colloidal properties, and sterilizing action towards environmental bacteria not involved in severe human infections needing novel treatments urgently, BPPB was never tested on clinically relevant MDR bacteria against which currently available antibiotics fail. Here, for the first time, the antibacterial activity of BPPB was investigated on fifty MDR clinical isolates of both Gram-positive and Gram-negative species responsible of serious human infections difficult to manage due to the complex pattern of resistance of pathogens. Results from MICs determination established that BPPB is active at low to very low MICs against all the species tested regardless of their worrying resistance. Moreover, it caused a 2 log CFU reduction in the initial inoculum after 6 hours of exposure in 24 h time killing experiments. The antibacterial activities of BPPB have been compared with that of several QPSs previously reported establishing the superiority of BPPB in almost all cases. Moreover, for the first time, the cytotoxicity of BPPB was investigated on human liver cells HepG2 and monkey kidney cells Cos-7 by carrying out MTT and LHD essays. Both essays evidenced similar pattern of toxicity and safety profiles at concentrations ≤ 5 μg/mL towards Cos-7 and ≤ 10 μg/mL towards HepG2 cells. Considering results obtained on HepG2 cells which are a better in vitro model for human biology, very high selectivity indices (SIs) > 10 were obtained against all MDR Gram-positive isolates considered and *E. coli*, while SIs = 1.4-5.6 were detected also on worrying Gram-negative species such as *A. baumannii* and *S. maltophylia*. This study also confirmed that antibacterial quaternary phosphonium salts (QPSs) could be more effective and less cytotoxic than ammonium counterpart (QASs), that *bis*-QPSs could be more potent antibacterials than mono-QPSs, that hindered QPSs such as TPP-based compounds could be more active and less cytotoxic than other QPSs and that bola-amphiphiles TPP-based molecules possess peculiar colloidal properties allowing them to self-assembling in nano micelles thus improving their biological effect as often observed for nanomaterials. Collectively, BPPB could therefore represent a novel potent template molecule to develop clinically applicable new antibacterial devices for counteracting infections sustained by antibiotic-resistant superbugs not manageable with currently available antibiotics. Future improvements in the antibacterial effects of PBBP while reducing its cytotoxic profiles further, could

derive by varying the length of the alkyl chain that acts as a linker between the two cationic heads, and therefore by the liposomal formulation of the most promising compounds using themselves as cationic lipids.

Supplementary Materials: The following supporting information can be downloaded at the website of this paper posted on Preprints.org. Figure S1. Optical micrograph of solid BPPB obtained using a 4 × objective; Figure S2. Size distribution of BPPB vesicles and large aggregates self-formed in a 10 mM solution; Figure S3. Size distribution of BPPB vesicles and aggregates self-formed in a 5 mM solution. Figure S4. Size distributions of BPPB vesicles and aggregates self-formed in a 5 mM solution. Figure S5. Cells viability (%) of Cos-7 (blue trace) and HepG2 (green trace) cells vs increasing BPPB concentrations (0.5-100 μg/mL) after 24 hours of exposure. Concentration = 0.0 μg/mL corresponded to the control. Figure S6. Cytotoxicity (LDH release OD) on Cos-7 (blue trace) and HepG2 (green trace) cells vs increasing BPPB concentrations (0.5-100 μg/mL) after 24 hours of exposure. Concentration = 0.0 μg/mL corresponded to the control. Figure S7. Plot of Log concentration of PBBP vs. cell viability (%) (blue and green traces with indicators and error bars) and plot of nonlinear fit of Log concentrations of PBBP vs. cell viability (%) (blue and green traces without indicators).

Author Contributions: Conceptualization, S.A., A.M.S. and M.M.; methodology, software, validation, formal analysis, investigation, resources, data curation, writing—original draft preparation, visualization, supervision, and project administration, S.A. (for the part of synthesis and characterization of all chemicals present in the study), A.M.S. and G.P. (for all the microbiology), M.M., C.T. and F.B. (for the biological experiments on human cells). DLS analyses, G.Z. Writing—review and editing, S.A., A.M.S., M.M., C.S., G.Z. and C.M.A. All authors have read and agreed to the published version of the manuscript.

Funding: This research received no external funding.

Data Availability Statement: All necessary data are comprised in this manuscript and in the related Supplementary Materials.

Acknowledgments: The authors thank IRCCS Istituto Giannina Gaslini, who putted at our disposition the DLS analyses instrument, Paolo Olivieri for the ATR-FTIR analyses and Paolo Giordani for optical microscopy investigations.

Institutional Review Board Statement: Not applicable.

Informed Consent Statement: Not applicable.

Conflicts of Interest: The authors declare no conflict of interest.

References

1. Ermolaev, V. V.; Arkhipova, D.M.; Miluykov, V.A.; Lyubina, A.P.; Amerhanova, S.K.; Kulik, N. V.; Voloshina, A.D.; Ananikov, V.P. Sterically Hindered Quaternary Phosphonium Salts (QPSs): Antimicrobial Activity and Hemolytic and Cytotoxic Properties. *Int J Mol Sci* **2021**, *23*, 86, doi:10.3390/ijms23010086.
2. Saliba, R.; Zahar, J.-R.; Dabar, G.; Riachy, M.; Karam-Sarkis, D.; Husni, R. Limiting the Spread of Multidrug-Resistant Bacteria in Low-to-Middle-Income Countries: One Size Does Not Fit All. *Pathogens* **2023**, *12*, 144, doi:10.3390/pathogens12010144.
3. Dryden, M. Reactive Oxygen Species: A Novel Antimicrobial. *Int J Antimicrob Agents* **2018**, *51*, 299–303, doi:10.1016/j.ijantimicag.2017.08.029.
4. Davis, S.C.; Martinez, L.; Kirsner, R. The Diabetic Foot: The Importance of Biofilms and Wound Bed Preparation. *Curr Diab Rep* **2006**, *6*, 439–445, doi:10.1007/s11892-006-0076-x.
5. Alfei, S.; Caviglia, D. Prevention and Eradication of Biofilm by Dendrimers: A Possibility Still Little Explored. *Pharmaceutics* **2022**, *14*, 2016, doi:10.3390/pharmaceutics14102016.
6. Ye, J.; Chen, X. Current Promising Strategies against Antibiotic-Resistant Bacterial Infections. *Antibiotics* **2022**, *12*, 67, doi:10.3390/antibiotics12010067.
7. Richter, S.G.; Elli, D.; Kim, H.K.; Hendrickx, A.P.A.; Sorg, J.A.; Schneewind, O.; Missiakas, D. Small Molecule Inhibitor of Lipoteichoic Acid Synthesis Is an Antibiotic for Gram-Positive Bacteria. *Proceedings of the National Academy of Sciences* **2013**, *110*, 3531–3536, doi:10.1073/pnas.1217337110.
8. Alfei, S.; Schito, G.C.; Schito, A.M.; Zuccari, G. ..Reactive Oxygen Species (ROS)-Mediated Antibacterial Oxidative Therapies: Available Methods to Generate ROS and a Novel Option Proposal. *IJMS* **2024**, 2024051628.
9. Dryden, M. Reactive Oxygen Therapy: A Novel Therapy in Soft Tissue Infection. *Curr Opin Infect Dis* **2017**, *30*, 143–149, doi:10.1097/QCO.0000000000000350.

10. Dryden, M.S.; Cooke, J.; Salib, R.J.; Holding, R.E.; Biggs, T.; Salamat, A.A.; Allan, R.N.; Newby, R.S.; Halstead, F.; Oppenheim, B.; et al. Reactive Oxygen: A Novel Antimicrobial Mechanism for Targeting Biofilm-Associated Infection. *J Glob Antimicrob Resist* **2017**, *8*, 186–191, doi:10.1016/j.jgar.2016.12.006.
11. Dunnill, C.; Patton, T.; Brennan, J.; Barrett, J.; Dryden, M.; Cooke, J.; Leaper, D.; Georgopoulos, N.T. Reactive Oxygen Species (ROS) and Wound Healing: The Functional Role of ROS and Emerging ROS-modulating Technologies for Augmentation of the Healing Process. *Int Wound J* **2017**, *14*, 89–96, doi:10.1111/iwj.12557.
12. Bacchetti, F.; Schito, A.M.; Milanese, M.; Castellaro, S.; Alfei, S. Anti Gram-Positive Bacteria Activity of Synthetic Quaternary Ammonium Lipid and Its Precursor Phosphonium Salt. *Int J Mol Sci* **2024**, *25*, 2761, doi:10.3390/ijms25052761.
13. Lei, Y.; Zhou, S.; Dong, C.; Zhang, A.; Lin, Y. PDMS Tri-Block Copolymers Bearing Quaternary Ammonium Salts for Epidermal Antimicrobial Agents: Synthesis, Surface Adsorption and Non-Skin-Penetration. *React Funct Polym* **2018**, *124*, 20–28, doi:10.1016/j.reactfunctpolym.2018.01.007.
14. Jiao, Y.; Niu, L.; Ma, S.; Li, J.; Tay, F.R.; Chen, J. Quaternary Ammonium-Based Biomedical Materials: State-of-the-Art, Toxicological Aspects and Antimicrobial Resistance. *Prog Polym Sci* **2017**, *71*, 53–90, doi:10.1016/j.progpolymsci.2017.03.001.
15. Zhou, C.; Wang, Y. Structure–Activity Relationship of Cationic Surfactants as Antimicrobial Agents. *Curr Opin Colloid Interface Sci* **2020**, *45*, 28–43, doi:10.1016/j.cocis.2019.11.009.
16. Costa, S.P.F.; Azevedo, A.M.O.; Pinto, P.C.A.G.; Saraiva, M.L.M.F.S. Environmental Impact of Ionic Liquids: Recent Advances in (Eco)Toxicology and (Bio)Degradability. *ChemSusChem* **2017**, *10*, 2321–2347, doi:10.1002/cssc.201700261.
17. Alfei, S.; Piatti, G.; Caviglia, D.; Schito, A. Synthesis, Characterization, and Bactericidal Activity of a 4-Ammoniumbuthylstyrene-Based Random Copolymer. *Polymers (Basel)* **2021**, *13*, 1140, doi:10.3390/polym13071140.
18. Zhou, Z.; Zhou, S.; Zhang, X.; Zeng, S.; Xu, Y.; Nie, W.; Zhou, Y.; Xu, T.; Chen, P. Quaternary Ammonium Salts: Insights into Synthesis and New Directions in Antibacterial Applications. *Bioconjug Chem* **2023**, *34*, 302–325, doi:10.1021/acs.bioconjchem.2c00598.
19. Schito, A.M.; Piatti, G.; Caviglia, D.; Zuccari, G.; Alfei, S. Broad-Spectrum Bactericidal Activity of a Synthetic Random Copolymer Based on 2-Methoxy-6-(4-Vinylbenzyloxy)-Benzylammonium Hydrochloride. *Int J Mol Sci* **2021**, *22*, 5021, doi:10.3390/ijms22095021.
20. Alfei, S. Shifting from Ammonium to Phosphonium Salts: A Promising Strategy to Develop Next-Generation Weapons against Biofilms. *Pharmaceutics* **2024**, *16*, 80, doi:10.3390/pharmaceutics16010080.
21. De Oliveira, D.M.P.; Forde, B.M.; Kidd, T.J.; Harris, P.N.A.; Schembri, M.A.; Beatson, S.A.; Paterson, D.L.; Walker, M.J. Antimicrobial Resistance in ESKAPE Pathogens. *Clin Microbiol Rev* **2020**, *33*, doi:10.1128/CMR.00181-19.
22. Jiao, Y.; Niu, L.; Ma, S.; Li, J.; Tay, F.R.; Chen, J. Quaternary Ammonium-Based Biomedical Materials: State-of-the-Art, Toxicological Aspects and Antimicrobial Resistance. *Prog Polym Sci* **2017**, *71*, 53–90, doi:10.1016/j.progpolymsci.2017.03.001.
23. Zhang, C.; Cui, F.; Zeng, G.; Jiang, M.; Yang, Z.; Yu, Z.; Zhu, M.; Shen, L. Quaternary Ammonium Compounds (QACs): A Review on Occurrence, Fate and Toxicity in the Environment. *Science of The Total Environment* **2015**, *518–519*, 352–362, doi:10.1016/j.scitotenv.2015.03.007.
24. Telesiński, A.; Pawłowska, B.; Biczak, R.; Śnieg, M.; Wróbel, J.; Dunikowska, D.; Meller, E. Enzymatic Activity and Its Relationship with Organic Matter Characterization and Ecotoxicity to Aliivibrio Fischeri of Soil Samples Exposed to Tetrabutylphosphonium Bromide. *Sensors* **2021**, *21*, 1565, doi:10.3390/s21051565.
25. Kimmig, J.; Jerchel, D. Die Wirkung von Invertseifen Auf Die Durch Pilze Und Kokken Bedingten Hautkrankheiten. *Klin Wochenschr* **1950**, *28*, 429–431, doi:10.1007/BF01485528.
26. Kanazawa, A.; Ikeda, T.; Endo, T. Synthesis and Antimicrobial Activity of Dimethyl- and Trimethyl-Substituted Phosphonium Salts with Alkyl Chains of Various Lengths. *Antimicrob Agents Chemother* **1994**, *38*, 945–952, doi:10.1128/AAC.38.5.945.
27. Alfei, S.; Schito, A.M. Positively Charged Polymers as Promising Devices against Multidrug Resistant Gram-Negative Bacteria: A Review. *Polymers (Basel)* **2020**, *12*, 1195, doi:10.3390/polym12051195.
28. Bachowska, B.; Kazmierczak-Baranska, J.; Cieslak, M.; Nawrot, B.; Szczęsna, D.; Skalik, J.; Bałczewski, P. High Cytotoxic Activity of Phosphonium Salts and Their Complementary Selectivity towards HeLa and K562 Cancer Cells: Identification of Tri- *n* -butyl- *n* -hexadecylphosphonium Bromide as a Highly Potent Anti-HeLa Phosphonium Salt. *ChemistryOpen* **2012**, *1*, 33–38, doi:10.1002/open.201100003.
29. Alfei, S. Cationic Materials for Gene Therapy: A Look Back to the Birth and Development of 2,2-Bis-(Hydroxymethyl)Propanoic Acid-Based Dendrimer Scaffolds. *Int J Mol Sci* **2023**, *24*, 16006, doi:10.3390/ijms242116006.
30. Pugachev, M. V.; Shtyrlin, N. V.; Sysoeva, L.P.; Nikitina, E. V.; Abdullin, T.I.; Iksanova, A.G.; Ilaeva, A.A.; Musin, R.Z.; Berdnikov, E.A.; Shtyrlin, Y.G. Synthesis and Antibacterial Activity of Novel Phosphonium Salts on the Basis of Pyridoxine. *Bioorg Med Chem* **2013**, *21*, 4388–4395, doi:10.1016/j.bmc.2013.04.051.

31. Cieniecka-Rosłonkiewicz, A.; Pernak, J.; Kubis-Feder, J.; Ramani, A.; Robertson, A.J.; Seddon, K.R. Synthesis, Anti-Microbial Activities and Anti-Electrostatic Properties of Phosphonium-Based Ionic Liquids. *Green Chemistry* **2005**, *7*, 855, doi:10.1039/b508499g.
32. Bedard, J.; Caschera, A.; Foucher, D.A. Access to Thermally Robust and Abrasion Resistant Antimicrobial Plastics: Synthesis of UV-Curable Phosphonium Small Molecule Coatings and Extrudable Additives. *RSC Adv* **2021**, *11*, 5548–5555, doi:10.1039/D1RA00555C.
33. Süer, N.C.; Demir, C.; Ünübol, N.A.; Yalçın, Ö.; Kocagöz, T.; Eren, T. Antimicrobial Activities of Phosphonium Containing Polynorbornenes. *RSC Adv* **2016**, *6*, 86151–86157, doi:10.1039/C6RA15545F.
34. Yuan, B.; Hu, W.; Lv, S.; Huang, J.; Huang, K. Synthesis of Aliphatic Symmetric Diphosphonium Salts and Bactericidal Activity of Selected Products. *Chemistry Journal of Moldova* **2017**, *12*, 81–86, doi:10.19261/cjm.2017.376.
35. Wei, W.; Yuan, B.; Lv, S.; Liao, Q.; Huang, J. Synthesis, Characterization and Performance of a New Type of Alkylene Triphenyl Double Quaternary Phosphonium Salt. *Journal of Materials Science and Chemical Engineering* **2013**, *01*, 61–65, doi:10.4236/msce.2013.15013.
36. Pugachev, M. V.; Shtyrlin, N. V.; Sapozhnikov, S. V.; Sysoeva, L.P.; Iksanova, A.G.; Nikitina, E. V.; Musin, R.Z.; Lodochnikova, O.A.; Berdnikov, E.A.; Shtyrlin, Y.G. Bis-Phosphonium Salts of Pyridoxine: The Relationship between Structure and Antibacterial Activity. *Bioorg Med Chem* **2013**, *21*, 7330–7342, doi:10.1016/j.bmc.2013.09.056.
37. Lei, Q.; Lai, X.; Zhang, Y.; Li, Z.; Li, R.; Zhang, W.; Ao, N.; Zhang, H. PEGylated Bis-Quaternary Triphenyl-Phosphonium Tosylate Allows for Balanced Antibacterial Activity and Cytotoxicity. *ACS Appl Bio Mater* **2020**, *3*, 6400–6407, doi:10.1021/acsabm.0c00837.
38. Ceccacci, F.; Sennato, S.; Rossi, E.; Proroga, R.; Sarti, S.; Diociaiuti, M.; Casciardi, S.; Mussi, V.; Ciogli, A.; Bordi, F.; et al. Aggregation Behaviour of Triphenylphosphonium Bolaamphiphiles. *J Colloid Interface Sci* **2018**, *531*, 451–462, doi:10.1016/j.jcis.2018.07.067.
39. Alfei, S.; Caviglia, D.; Piatti, G.; Zuccari, G.; Schito, A.M. Synthesis, Characterization and Broad-Spectrum Bactericidal Effects of Ammonium Methyl and Ammonium Ethyl Styrene-Based Nanoparticles. *Nanomaterials* **2022**, *12*, 2743, doi:10.3390/nano12162743.
40. Alfei, S.; Castellaro, S.; Taptue, G.B. Synthesis and NMR Characterization of Dendrimers Based on 2, 2-Bis-(Hydroxymethyl)-Propanoic Acid (Bis-HMPA) Containing Peripheral Amino Acid Residues for Gene Transfection. *Organic Communications* **2017**, *10*, 144–177, doi:10.25135/acg.oc.22.17.06.034.
41. Alfei, S.; Castellaro, S. Synthesis and Characterization of Polyester-Based Dendrimers Containing Peripheral Arginine or Mixed Amino Acids as Potential Vectors for Gene and Drug Delivery. *Macromol Res* **2017**, *25*, 1172–1186, doi:10.1007/s13233-017-5160-3.
42. Alfei, S.; Taptue, G.B.; Catena, S.; Bisio, A. Synthesis of Water-Soluble, Polyester-Based Dendrimer Prodrugs for Exploiting Therapeutic Properties of Two Triterpenoid Acids. *Chinese Journal of Polymer Science* **2018**, *36*, 999–1010, doi:10.1007/s10118-018-2124-9.
43. Pifer, C.W.; Wollish, E.G. Potentiometric Titration of Salts of Organic Bases in Acetic Acid. *Anal Chem* **1952**, *24*, 300–306, doi:10.1021/ac60062a011.
44. EUCAST. European Committee on Antimicrobial Susceptibility Testing. Available Online: Https://Www.Eucast.Org/Ast_of_bacteria/ (Accessed on 20 January 2024). .
45. Schito, A.M.; Piatti, G.; Stauder, M.; Bisio, A.; Giacomelli, E.; Romussi, G.; Pruzzo, C. Effects of Demethylfruticuline A and Fruticuline A from Salvia Corrugata Vahl. on Biofilm Production in Vitro by Multiresistant Strains of Staphylococcus Aureus, Staphylococcus Epidermidis and Enterococcus Faecalis. *Int J Antimicrob Agents* **2011**, *37*, 129–134, doi:10.1016/j.ijantimicag.2010.10.016.
46. Berridge, M. V.; Herst, P.M.; Tan, A.S. Tetrazolium Dyes as Tools in Cell Biology: New Insights into Their Cellular Reduction. In; 2005; pp. 127–152.
47. Kumar, P.; Nagarajan, A.; Uchil, P.D. Analysis of Cell Viability by the Lactate Dehydrogenase Assay. *Cold Spring Harb Protoc* **2018**, *2018*, pdb.prot095497, doi:10.1101/pdb.prot095497.
48. AVALOS, F.; ORTIZ, J.; ZITZUMBO, R.; LOPEZMANCHADO, M.; VERDEJO, R.; ARROYO, M. Phosphonium Salt Intercalated Montmorillonites. *Appl Clay Sci* **2009**, *43*, 27–32, doi:10.1016/j.clay.2008.07.008.
49. Daasch, L.; Smith, D. Infrared Spectra of Phosphorus Compounds. *Anal Chem* **1951**, *23*, 853–868, doi:10.1021/ac60054a008.
50. Arkhipova, D.M.; Samigullina, A.I.; Minyaev, M.E.; Lyubina, A.P.; Voloshina, A.D.; Ermolaev, V. V. Synthesis, Crystal Structure, and Biological Activity of Menthol-Based Chiral Quaternary Phosphonium Salts (CQPSs). *Struct Chem* **2024**, *35*, 75–88, doi:10.1007/s11224-023-02259-0.
51. Galkina, I. V.; Andriyashin, V. V.; Romanov, S.R.; Egorova, S.N.; Vorob'eva, N. V.; Shulaeva, M.P.; Pozdeev, O.K.; Litvinov, I.A.; Bakhtiyarova, Y. V. Synthesis, Structure and Antimicrobial Activity of Sterically Hindered Bis-Phosphonium Derivatives of 2,6-Di-Tert-Butyl-4-Methylphenol. *Mendeleev Communications* **2023**, *33*, 635–637, doi:10.1016/j.mencom.2023.09.014.

52. Akshay Ravindra, P.; Karpagam, S. Synthesis and Biological Activity of Azine Heterocycle Functionalized Quaternary Phosphonium Salts. *IOP Conf Ser Mater Sci Eng* **2017**, *263*, 022017, doi:10.1088/1757-899X/263/2/022017.
53. Kratochvil, Byron. Titrations in Nonaqueous Solvents. *Anal Chem* **1982**, *54*, 105–121, doi:10.1021/ac00242a011.
54. Seher, A. Dr. I. Gyenes, C. Sc. (Chim.), Titrationen in Nichtwäßrigen Medien, 3. Neubearb. u. Erg. Aufl., 701 S., 206 Abb., 108 Tab., Gln., Ferdinand Enke Verlag, Stuttgart 1970, Preis: 84.—DM. *Fette, Seifen, Anstrichmittel* **1973**, *75*, 232–232, doi:10.1002/lipi.19730750404.
55. Šafařík, L.; Stránský, Z.; Svehla, G.; Burns, D.T. Titrimetric Analysis in Organic Solvents (Comprehensive Analytical Chemistry, Vol. XXII). *Anal Chim Acta* **1987**, *201*, 367, doi:10.1016/S0003-2670(00)85367-2.
56. Mascellani, Giuseppe.; Casalini, Claudio. Use of Mercuric Acetate in Potentiometric Titrations in a Nonaqueous Medium. *Anal Chem* **1975**, *47*, 2468–2470, doi:10.1021/ac60364a040.
57. Kan, P.L.; Papahadjopoulos-Sternberg, B.; Wong, D.; Waigh, R.D.; Watson, D.G.; Gray, A.I.; McCarthy, D.; McAllister, M.; Schätzlein, A.G.; Uchegbu, I.F. Highly Hydrophilic Fused Aggregates (Microsponges) from a C12 Spermine Bolaamphiphile. *J Phys Chem B* **2004**, *108*, 8129–8135, doi:10.1021/jp0372237.
58. Franceschi, S.; Andreu, V.; de Viguerie, N.; Riviere, M.; Lattes, A.; Moisand, A. Synthesis and Aggregation Behaviour of Two-Headed Surfactants Containing the Urocanic Acid Moiety. *New Journal of Chemistry* **1998**, *22*, 225–231, doi:10.1039/a708326b.
59. Weissig, V.; Torchilin, V.P. Cationic Bolasomes with Delocalized Charge Centers as Mitochondria-Specific DNA Delivery Systems. *Adv Drug Deliv Rev* **2001**, *49*, 127–149, doi:10.1016/S0169-409X(01)00131-4.
60. Alfei, S.; Marengo, B.; Domenicotti, C. Polyester-Based Dendrimer Nanoparticles Combined with Etoposide Have an Improved Cytotoxic and Pro-Oxidant Effect on Human Neuroblastoma Cells. *Antioxidants* **2020**, *9*, 50, doi:10.3390/antiox9010050.
61. Alfei, S.; Zuccari, G.; Caviglia, D.; Brullo, C. Synthesis and Characterization of Pyrazole-Enriched Cationic Nanoparticles as New Promising Antibacterial Agent by Mutual Cooperation. *Nanomaterials* **2022**, *12*, 1215, doi:10.3390/nano12071215.
62. Alfei, S.; Caviglia, D.; Piatti, G.; Zuccari, G.; Schito, A.M. Synthesis, Characterization and Broad-Spectrum Bactericidal Effects of Ammonium Methyl and Ammonium Ethyl Styrene-Based Nanoparticles. *Nanomaterials* **2022**, *12*, 2743, doi:10.3390/nano12162743.
63. Alfei, S.; Brullo, C.; Caviglia, D.; Zuccari, G. Preparation and Physicochemical Characterization of Water-Soluble Pyrazole-Based Nanoparticles by Dendrimer Encapsulation of an Insoluble Bioactive Pyrazole Derivative. *Nanomaterials* **2021**, *11*, 2662, doi:10.3390/nano11102662.
64. Fröhlich, E. The Role of Surface Charge in Cellular Uptake and Cytotoxicity of Medical Nanoparticles. *Int J Nanomedicine* **2012**, 5577, doi:10.2147/IJN.S36111.
65. Alfei, S.; Spallarossa, A.; Lusardi, M.; Zuccari, G. Successful Dendrimer and Liposome-Based Strategies to Solubilize an Antiproliferative Pyrazole Otherwise Not Clinically Applicable. *Nanomaterials* **2022**, *12*, 233, doi:10.3390/nano12020233.
66. Petri-Fink, A.; Chastellain, M.; Juillerat-Jeanneret, L.; Ferrari, A.; Hofmann, H. Development of Functionalized Superparamagnetic Iron Oxide Nanoparticles for Interaction with Human Cancer Cells. *Biomaterials* **2005**, *26*, 2685–2694, doi:10.1016/j.biomaterials.2004.07.023.
67. Jambhrunkar, S.; Yu, M.; Yang, J.; Zhang, J.; Shrotri, A.; Endo-Munoz, L.; Moreau, J.; Lu, G.; Yu, C. Stepwise Pore Size Reduction of Ordered Nanoporous Silica Materials at Angstrom Precision. *J Am Chem Soc* **2013**, *135*, 8444–8447, doi:10.1021/ja402463h.
68. Chen, L.; Mccrate, J.M.; Lee, J.C.-M.; Li, H. The Role of Surface Charge on the Uptake and Biocompatibility of Hydroxyapatite Nanoparticles with Osteoblast Cells. *Nanotechnology* **2011**, *22*, 105708, doi:10.1088/0957-4484/22/10/105708.
69. Akinc, A.; Battaglia, G. Exploiting Endocytosis for Nanomedicines. *Cold Spring Harb Perspect Biol* **2013**, *5*, a016980–a016980, doi:10.1101/cshperspect.a016980.
70. Mondal, A.H.; Khare, K.; Saxena, P.; Debnath, P.; Mukhopadhyay, K.; Yadav, D. A Review on Colistin Resistance: An Antibiotic of Last Resort. *Microorganisms* **2024**, *12*, 772, doi:10.3390/microorganisms12040772.
71. Silva, J.T.; López-Medrano, F. Cefiderocol, a New Antibiotic against Multidrug-Resistant Gram-Negative Bacteria. *Rev Esp Quimioter* **2021**, *34 Suppl 1*, 41–43, doi:10.37201/req/s01.12.2021.
72. Karakonstantis, S.; Rousaki, M.; Kritsotakis, E.I. Cefiderocol: Systematic Review of Mechanisms of Resistance, Heteroresistance and In Vivo Emergence of Resistance. *Antibiotics* **2022**, *11*, 723, doi:10.3390/antibiotics11060723.
73. Alfei, S.; Schito, A.M. β-Lactam Antibiotics and β-Lactamase Enzymes Inhibitors, Part 2: Our Limited Resources. *Pharmaceuticals* **2022**, *15*, 476, doi:10.3390/ph15040476.
74. Alfei, S.; Zuccari, G. Recommendations to Synthetize Old and New β-Lactamases Inhibitors: A Review to Encourage Further Production. *Pharmaceuticals* **2022**, *15*, 384, doi:10.3390/ph15030384.

75. Schito, A.M.; Piatti, G.; Caviglia, D.; Zuccari, G.; Zorzoli, A.; Marimpietri, D.; Alfei, S. Bactericidal Activity of Non-Cytotoxic Cationic Nanoparticles against Clinically and Environmentally Relevant Pseudomonas Spp. Isolates. *Pharmaceutics* **2021**, *13*, 1411, doi:10.3390/pharmaceutics13091411.
76. De Oliveira, D.M.P.; Forde, B.M.; Kidd, T.J.; Harris, P.N.A.; Schembri, M.A.; Beatson, S.A.; Paterson, D.L.; Walker, M.J. Antimicrobial Resistance in ESKAPE Pathogens. *Clin Microbiol Rev* **2020**, *33*, doi:10.1128/CMR.00181-19.
77. García-Solache, M.; Rice, L.B. The Enterococcus: A Model of Adaptability to Its Environment. *Clin Microbiol Rev* **2019**, *32*, doi:10.1128/CMR.00058-18.
78. Levitus, M.; Rewane, A.; Perera, T.B. *Vancomycin-Resistant Enterococci*; 2024;
79. Chiang, H.-Y.; Perencevich, E.N.; Nair, R.; Nelson, R.E.; Samore, M.; Khader, K.; Chorazy, M.L.; Herwaldt, L.A.; Blevins, A.; Ward, M.A.; et al. Incidence and Outcomes Associated With Infections Caused by Vancomycin-Resistant Enterococci in the United States: Systematic Literature Review and Meta-Analysis. *Infect Control Hosp Epidemiol* **2017**, *38*, 203–215, doi:10.1017/ice.2016.254.
80. Miller, W.R.; Murray, B.E.; Rice, L.B.; Arias, C.A. Vancomycin-Resistant Enterococci. *Infect Dis Clin North Am* **2016**, *30*, 415–439, doi:10.1016/j.idc.2016.02.006.
81. Fernández-Hidalgo, N.; Escolà-Vergé, L. Enterococcus Faecalis Bacteremia. *J Am Coll Cardiol* **2019**, *74*, 202–204, doi:10.1016/j.jacc.2019.03.526.
82. Rosa, T.F.; Coelho, S.S.; Foletto, V.S.; Bottega, A.; Serafin, M.B.; Machado, C. de S.; Franco, L.N.; Paula, B.R.; Hörner, R. Alternatives for the Treatment of Infections Caused by ESKAPE Pathogens. *J Clin Pharm Ther* **2020**, *45*, 863–873, doi:10.1111/jcpt.13149.
83. Alfei, S.; Brullo, C.; Caviglia, D.; Piatti, G.; Zorzoli, A.; Marimpietri, D.; Zuccari, G.; Schito, A.M. Pyrazole-Based Water-Soluble Dendrimer Nanoparticles as a Potential New Agent against Staphylococci. *Biomedicines* **2021**, *10*, 17, doi:10.3390/biomedicines10010017.
84. Bozdogan, B. Antibacterial Susceptibility of a Vancomycin-Resistant Staphylococcus Aureus Strain Isolated at the Hershey Medical Center. *Journal of Antimicrobial Chemotherapy* **2003**, *52*, 864–868, doi:10.1093/jac/dkg457.
85. Tsiodras, S.; Gold, H.S.; Sakoulas, G.; Eliopoulos, G.M.; Wennersten, C.; Venkataraman, L.; Moellering, R.C.; Ferraro, M.J. Linezolid Resistance in a Clinical Isolate of Staphylococcus Aureus. *The Lancet* **2001**, *358*, 207–208, doi:10.1016/S0140-6736(01)05410-1.
86. Liu, C.; Bayer, A.; Cosgrove, S.E.; Daum, R.S.; Fridkin, S.K.; Gorwitz, R.J.; Kaplan, S.L.; Karchmer, A.W.; Levine, D.P.; Murray, B.E.; et al. Clinical Practice Guidelines by the Infectious Diseases Society of America for the Treatment of Methicillin-Resistant Staphylococcus Aureus Infections in Adults and Children. *Clinical Infectious Diseases* **2011**, *52*, e18–e55, doi:10.1093/cid/ciq146.
87. Nour El-Din, H.T.; Yassin, A.S.; Ragab, Y.M.; Hashem, A.M. Phenotype-Genotype Characterization and Antibiotic-Resistance Correlations Among Colonizing and Infectious Methicillin-Resistant Staphylococcus Aureus Recovered from Intensive Care Units. *Infect Drug Resist* **2021**, *Volume 14*, 1557–1571, doi:10.2147/IDR.S296000.
88. Breijyeh, Z.; Jubeh, B.; Karaman, R. Resistance of Gram-Negative Bacteria to Current Antibacterial Agents and Approaches to Resolve It. *Molecules* **2020**, *25*, 1340, doi:10.3390/molecules25061340.
89. Nunes, B.; Cagide, F.; Fernandes, C.; Borges, A.; Borges, F.; Simões, M. Efficacy of Novel Quaternary Ammonium and Phosphonium Salts Differing in Cation Type and Alkyl Chain Length against Antibiotic-Resistant Staphylococcus Aureus. *Int J Mol Sci* **2023**, *25*, 504, doi:10.3390/ijms25010504.
90. Wesevich, A.; Sutton, G.; Ruffin, F.; Park, L.P.; Fouts, D.E.; Fowler, V.G.; Thaden, J.T. Newly Named Klebsiella Aerogenes (Formerly Enterobacter Aerogenes) Is Associated with Poor Clinical Outcomes Relative to Other *Enterobacter* Species in Patients with Bloodstream Infection. *J Clin Microbiol* **2020**, *58*, doi:10.1128/JCM.00582-20.
91. Yahav, D.; Giske, C.G.; Grāmatniece, A.; Abodakpi, H.; Tam, V.H.; Leibovici, L. New β-Lactam–β-Lactamase Inhibitor Combinations. *Clin Microbiol Rev* **2020**, *34*, doi:10.1128/CMR.00115-20.
92. Karaiskos, I.; Galani, I.; Papoutsaki, V.; Galani, L.; Giamarellou, H. Carbapenemase Producing *Klebsiella Pneumoniae*: Implication on Future Therapeutic Strategies. *Expert Rev Anti Infect Ther* **2022**, *20*, 53–69, doi:10.1080/14787210.2021.1935237.
93. Rolston, K.V.I.; Safdar, A. Pseudomonas, Stenotrophomonas, Acinetobacter, and Other Nonfermentative Gram-Negative Bacteria and Medically Important Anaerobic Bacteria in Transplant Recipients. In *Principles and Practice of Transplant Infectious Diseases*; Springer New York: New York, NY, 2019; pp. 461–472.
94. Brooke, J.S. Advances in the Microbiology of Stenotrophomonas Maltophilia. *Clin Microbiol Rev* **2021**, *34*, doi:10.1128/CMR.00030-19.
95. Sommers, K.J.; Michaud, M.E.; Hogue, C.E.; Scharnow, A.M.; Amoo, L.E.; Petersen, A.A.; Carden, R.G.; Minbiole, K.P.C.; Wuest, W.M. Quaternary Phosphonium Compounds: An Examination of Non-Nitrogenous Cationic Amphiphiles That Evade Disinfectant Resistance. *ACS Infect Dis* **2022**, *8*, 387–397, doi:10.1021/acsinfecdis.1c00611.

96. Li, L.; Zhou, H.; Gai, F.; Chi, X.; Zhao, Y.; Zhang, F.; Zhao (Kent), Z. Synthesis of Quaternary Phosphonium N-Chloramine Biocides for Antimicrobial Applications. *RSC Adv* **2017**, *7*, 13244–13249, doi:10.1039/C6RA24954J.
97. Xuan, J.; Chen, S.; Ning, B.; Tolleson, W.H.; Guo, L. Development of HepG2-Derived Cells Expressing Cytochrome P450s for Assessing Metabolism-Associated Drug-Induced Liver Toxicity. *Chem Biol Interact* **2016**, *255*, 63–73, doi:10.1016/j.cbi.2015.10.009.
98. Donato, M.T.; Tolosa, L.; Gómez-Lechón, M.J. Culture and Functional Characterization of Human Hepatoma HepG2 Cells. *Methods Mol Biol* **2015**, *1250*, 77–93, doi:10.1007/978-1-4939-2074-7_5.
99. Tolosa, L.; Gómez-Lechón, M.J.; López, S.; Guzmán, C.; Castell, J. V; Donato, M.T.; Jover, R. Human Upcyte Hepatocytes: Characterization of the Hepatic Phenotype and Evaluation for Acute and Long-Term Hepatotoxicity Routine Testing. *Toxicol Sci* **2016**, *152*, 214–229, doi:10.1093/toxsci/kfw078.
100. Martínez-Sena, T.; Moro, E.; Moreno-Torres, M.; Quintás, G.; Hengstler, J.; Castell, J. V. Metabolomics-Based Strategy to Assess Drug Hepatotoxicity and Uncover the Mechanisms of Hepatotoxicity Involved. *Arch Toxicol* **2023**, *97*, 1723–1738, doi:10.1007/s00204-023-03474-8.
101. Donato, M.T.; Tolosa, L.; Gómez-Lechón, M.J. Culture and Functional Characterization of Human Hepatoma HepG2 Cells. In; 2015; pp. 77–93.
102. Arzumanian, V.A.; Kiseleva, O.I.; Poverennaya, E. V. The Curious Case of the HepG2 Cell Line: 40 Years of Expertise. *Int J Mol Sci* **2021**, *22*, 13135, doi:10.3390/ijms222313135.
103. Cushnie, T.P.T.; Cushnie, B.; Echeverría, J.; Fowsantear, W.; Thammawat, S.; Dodgson, J.L.A.; Law, S.; Clow, S.M. Bioprospecting for Antibacterial Drugs: A Multidisciplinary Perspective on Natural Product Source Material, Bioassay Selection and Avoidable Pitfalls. *Pharm Res* **2020**, *37*, 125, doi:10.1007/s11095-020-02849-1.